DETECTION, DIAGNOSTICS, AND CHARACTERIZATION OF VIRUS-LIKE ORGANISMS AND CONFORMATIONAL DISEASE-LIKE PROTEINS IN PLANTS

A DISSERTATION
SUBMITTED TO THE FACULTY OF
UNIVERSITY OF MINNESOTA
BY

SARA ANN BRATSCH

IN PARTIAL FULFILLMENT OF THE REQUIREMENTS
FOR THE DEGREE OF
DOCTOR OF PHILOSOPHY

ADVISER DR. BENHAM E. LOCKHART
CO-ADVISER DR. NEIL E. OLSZEWSKI

OCTOBER 2016

Acknowledgements

I would sincerely like to thank my co-advisers Drs. Benham Lockhart and Neil Olszewski for their encouragement and support of my research. Their extensive knowledge, enthusiasm, and devotedness were invaluable for the completion of my research.

I would also like to thank my parents and my partner for their understanding, patience, and support throughout the duration of my doctoral degree.

Abstract

The projects in this thesis all investigated virus-like organisms in agronomically important plants. Chapter one consists of reports describing viruses identified in new hosts or locations. *Tobacco rattle virus* (TRV) was identified in symptomatic *Phryma leptostachya* L, a native perennial, from plants in an uncultivated habitat and suggests that TRV may be endemic to North America. Since TRV is the causal organism of corky ringspot of potato this study raises the possibility that native perennial plants could serve as a potential reservoir to cause disease in potato. *Canna yellow mottle virus* was isolated for the first time from symptomatic *Canna indica* in Kenya. Cut flowers are a major agronomic crop of Kenya and growers should plant only virus indexed plants to limit losses from virus infection. *Orchid fleck virus* was confirmed by microscopy and sequence analysis for the first time in the United States in *Phalaenopsis hybrida*. Asymptomatic *P. hybrida* tested by one step reverse transcription polymerase chain reaction (RT-PCR) did not yield the expected product while a two step RT-PCR, creating cDNA first, yielded the expected product. This indicates the one step RT-PCR diagnostic test can yield false negatives for asymptomatic plants.

Chapter two describes the production of polyclonal antibodies for the detection of *Orchid fleck virus* (OFV). OFV is a mite transmitted virus and has been reported word wide. The previous project identified a need for a reliable, inexpensive method to detect OFV in plants use for propagation, breeding, conservatories, or virus indexing projects. Polyclonal antibodies were produced in rabbits against *Escherichia coli* expressed OFV phosphoprotein and matrix protein. The resulting antiserums were assayed in PTA-

ELISA and DAS-ELISA. OFV phosphoprotein antisera in PTA-ELISA readily differentiated between healthy and OFV infected orchid (*Phalaenopsis hybrida*) tissue. OFV matrix antisera in PTA-ELISA detected bacterially-expressed protein but did not differentiate between healthy or OFV infected tissue. The OFV phosphoprotein antiserum can be used by in PTA-ELISA to reliably detect OFV.

Chapter three describes the molecular and biological characterization of a new *Nepovirus* causing a leaf mottling disease in *Petunia hybrida*. The sequence of the majority of the genome was determined by next generation sequencing and the sequence of remainder of the genome was obtained using a 5' RACE amplification and RT-PCR using poly-A tail and virus specific primers. Due to phylogenetic relationship and sufficient genome dissimilarity to characterized viruses I propose the name of Petunia Chlorotic Mottle Virus for a new *Nepovirus*.

The fourth chapter describes characterization of filamentous virus-like particles in members of the *Asteraceae* plant family including sunflower, chrysanthemum, coneflower, gerbera daisy, and zinnia. The filaments were 7-10 nanometers in diameter and could exceed 3,000 nm in length. The N-terminal sequences of the major proteins associated with purified filaments from several species were nearly identical and shared homology with the kunitz soybean trypsin inhibitor (KTI) family of proteins. CID MS/MS sequencing of the major proteins of purified sunflower filaments also shared homology with a KTI sequence. A Western blot using antiserum prepared against recombinant sunflower KTI protein labeled the observable protein bands from sunflower

filaments. Filaments composed of a major protein of KTI have been found across the *Asteraceae* family but have not been observed in dandelion, thistle, or lettuce.

Table of Contents

List of Tables

Page

Chapter II

Chapter III

Chapter IV

List of Figures

Page

Chapter I

Chapter II.

Chapter III.

Chapter IV

Contributing author acknowledgements

I would like to acknowledge Jennifer E. Flynn, Department of Plant Pathology, University of Minnesota, St. Paul 55108, as a co-author for Chapter I "Detection of Tobacco Rattle Virus (TRV) in *Phryma leptostachya* L.: A new native plant host in Minnesota".

I would like to also acknowledge Dr. Therese Atcham Agneroh, Department Agriculture and Animal Resources, National Polytechnic Institute Felix Houphouet Boigny (INP-HB), P.O. Box 1313 Yamoussoukro, Ivory Coast, as a co-author for Chapter I "First Report of Canna Yellow Mottle Virus in Kenya".

Finally I would like to acknowledge Dr. Carol Ishimaru, Department of Plant Pathology, University of Minnesota, St. Paul 55108, as a co-author for Chapter I "Confirmation of First Report of *Orchid fleck virus* in *Phalaenopsis* Hybrid Orchids in the USA". Dr. Ishimaru assisted with the bacterial pathogen exploratory experiments.

Chapter I.

Detection of Tobacco Rattle Virus (TRV) in *Phryma leptostachya* L.: A new native plant host in Minnesota

doi:10.1094/PHP-BR-14-0021

Phryma leptostachya L. (American Lopseed) is a native woodland perennial found throughout most of the United States and eastern Canadian provinces. Green leaves of *P. leptostachya* L. exhibiting yellow concentric line patterns and chlorotic dappling were observed on plants growing in an undisturbed area with no history of cultivation in Coon Rapids, Minnesota in July, 2013 (Figure 1). These symptoms were associated with infection by *Tobacco rattle virus* (TRV), which was identified by particle morphology, immunosorbent electron microscopy (ISEM), and sequencing of the immunocapture reverse transcription (RT)-PCR product. TRV is a Tobravirus consisting of rod shaped particles with a diameter of 21.3-23.1 nanometers (nm) and two particle lengths of 180-215 nm plus 46.0-115 nm (King 2011).

Transmission electron microscopy (TEM) observations of negatively stained, partially purified leaf tissue extracts (Ahlawat et al 1996) revealed rigid, rod-shaped virus-like particles similar to those of TRV and other tobraviruses. Particles had a width of 21.2-23.0 nm and length from 61.4 to 216.1 nm. These virus-like particles were confirmed to be those of TRV by ISEM (Ahlawat et al 1996) using antiserum to TRV (ATCC PVAS 75) (Figure 2). Immunocapture RT-PCR using the same antiserum with Ready-To-Go RT-PCR Beads (GE Healthcare UK Limited, UK) and oligonucleotide primers (Robinson 1992) generated the expected 464 bp product corresponding to the 16

kDa protein of RNA1 (Figure 3). This product was ligated, cloned (pGEM-T Easy Vector System; Promega, USA) and sequenced (MCLAB, San Francisco California). Raw sequences were assembled into a 464 bp consensus sequence (Sequencher, Gene Codes Corporation, MI, USA) and deposited in GenBank under accession number KJ937665.

Figure 1. Varied symptoms of TRV-infected *Phryma leptostachya* L., American Lopseed: A chlorotic dappling symptoms; B and C concentric line pattern symptoms.

The resulting sequence had 94% nucleotide sequence identity to published TRV sequences (AJ586803.1, JF935233.1). On the basis of virion morphology, ISEM, and

sequence identity, the virus associated with yellow concentric line patterns in *P. leptostachya* L. was identified as an isolate of TRV. To our knowledge, this is the first report of TRV infection in *P. leptostachya* L.

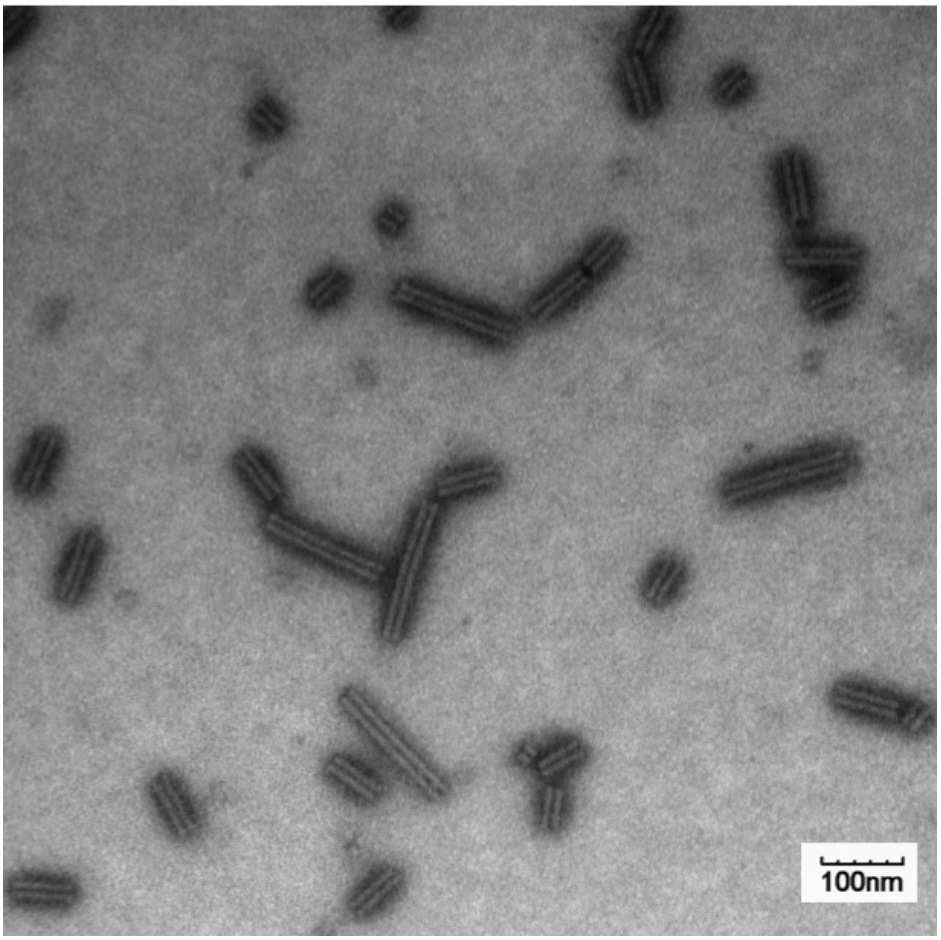

Figure 2. Immunosorbent electron microscopy of partially purified symptomatic *Phryma leptostachya* L. leaves showing antibody-decorated TRV particles stained with phosphotungstic acid at 66,000 times magnification.

TRV has previously been suggested to be an introduced, exotic pathogen in the United States. However, TRV is known to occur in native and ornamental perennials in Minnesota and Wisconsin habitats with no known history of crop cultivation (Lockhart & Mason 2011; Lockhart & Mason 2010; Lockhart 2000). The TRV isolate from *P.*

leptostachya L. has 94% nucleotide similarity to an isolate of TRV obtained from a hosta growing in an uncultivated forest (JF935233), 93% similarity to a Sherburn county potato isolate of TRV (JF935235), and 90% similarity to TRV isolated from *Hepatica acutiloba* (sharp-loped hepatica) in St. Cloud (JF935236).

The repeated isolation of TRV from plants in isolated, uncultivated habitats suggests that TRV may be endemic to North America (Lockhart & Mason 2011; Lockhart & Mason 2010; Lockhart 2000). TRV is the causal organism of corky ringspot of potato and further studies are needed to determine if infected native perennial plants could serve as a potential TRV reservoir that could infect potato.

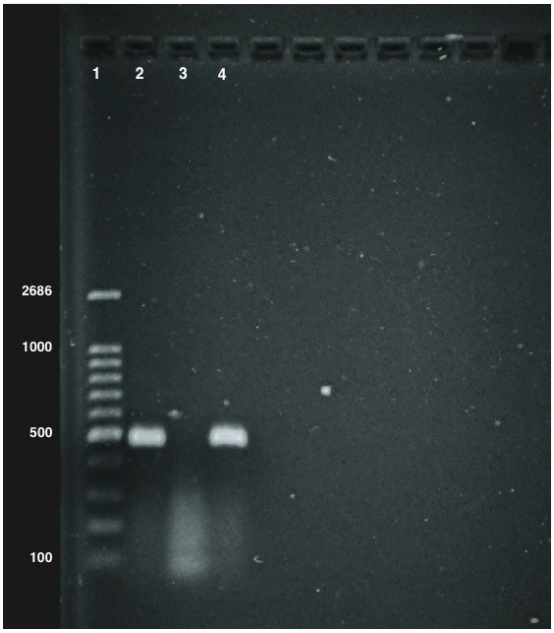

Figure 3. Immunocapture RT-PCR of TRV in symptomatic *Phryma leptostachya* using the primer pair A+B designed by Robinson (1992). Fisher Scientific 100 base pair ladder at left (lane 1), positive control from TRV infected *Nicotiana benthamiana* (lane 2), negative control from healthy *P. leptostachya* (lane 3), 464 base pair amplicon from symptomatic *P. leptostachya* (lane 4).

First Report of Canna yellow mottle virus in Kenya

doi:10.1094/PHP-BR-14-0037

Kenya is an important exporter of cut flowers for the European markets. During surveys conducted in April 2014, canna plants (*Canna indica*) were observed with distinctly different virus-like symptoms in two regions of Kenya. Leaves collected in Nairobi had yellow/green chlorotic mottle, necrotic mottle and veinal streaking symptoms (Figure 4). This sample was designated K1. Leaves collected in Kericho had green mosaic symptoms (Figure 4), and this sample was designated K2.

Both samples were examined by transmission electron microscopy (TEM) and immunosorbent electron microscopy (ISEM) for the presence of the viruses known to occur in cannas. These are: *Canna yellow mottle virus* (CaYMV), *Canna yellow streak virus* (CaYSV), *Bean yellow mosaic virus* (BYMV), a potyvirus resembling CaYSV (personal communication B. Lockhart), *Cucumber mosaic virus* (CMV), and *Tomato aspermy virus* (TAV). TEM observations of negatively stained, partially purified leaf tissue extracts (Ahlawat et al 1996) from K1 and K2 detected only bacilliform particles, with an approximate diameter of 30 nm and length of 120 nm, typical of CaYMV. No particles were observed in samples from non-symptomatic plants. Trapping and decoration of particles by ISEM (Ahlawat et al 1996) using a polyvalent antiserum raised against a mixture of isolates of *Sugarcane bacilliform virus* and *Banana streak virus* showed typical badnavirus-like particles from both K1 and K2 (Figure 5). No surveys were completed to determine the percent incidence of CaYMV in Kenya.

Figure 4. Typical symptoms found in cannas in Nairobi, left (K1) with yellow/green chlorotic mottle, necrotic mottle and veinal streaking symptoms. Leaves collected in Kericho, right (K2) had green mosaic symptoms.

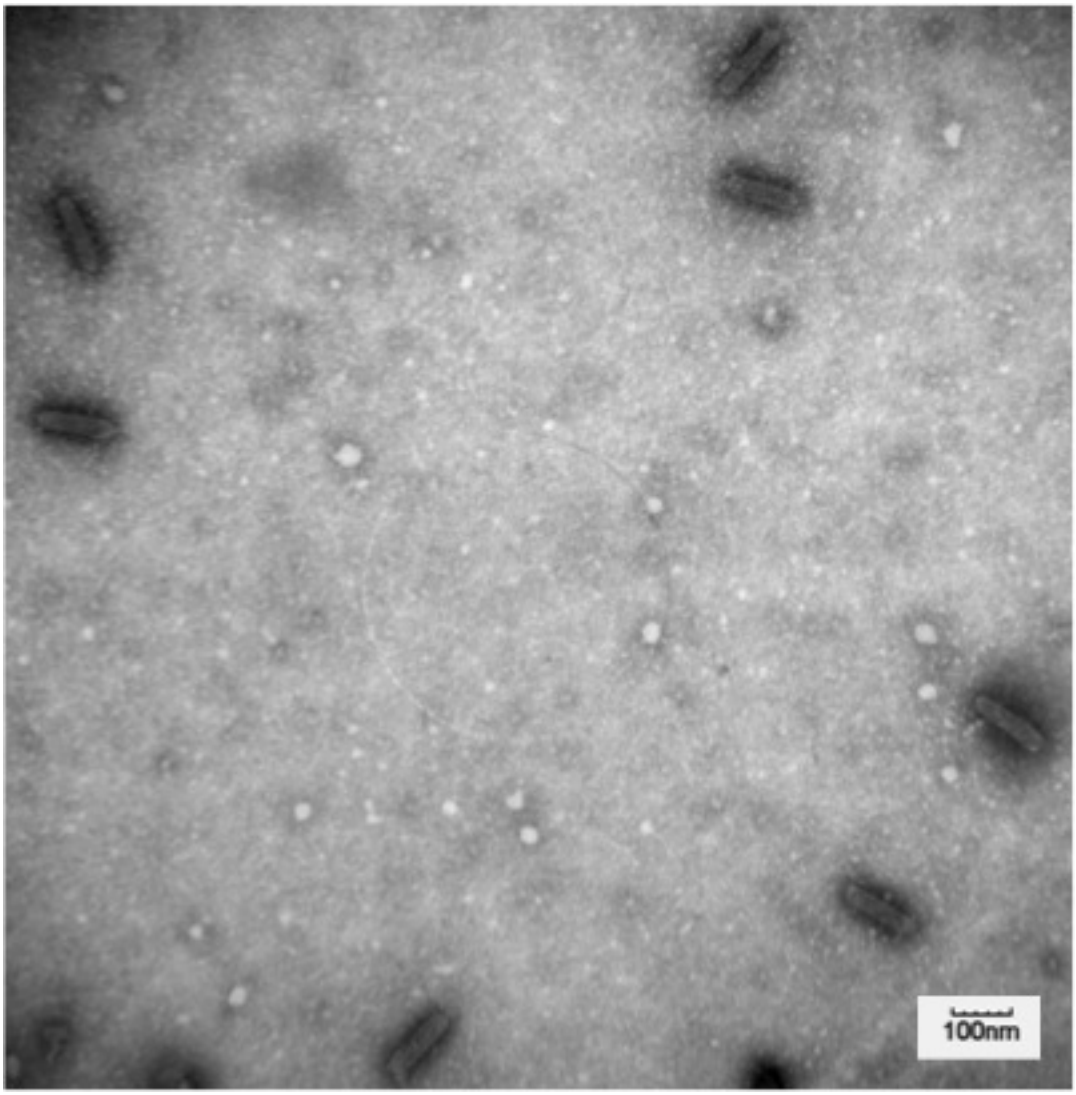

Figure 5. Immunosorbent electron microscopy (ISEM) of partially purified symptomatic canna leaves showing antibody decorated *Canna yellow mottle virus* particles stained with phosphotungstic acid at 53,000 times magnification.

The presence of CaYMV in the leaves of the two Kenyan isolates was confirmed by PCR using CaYMV-specific primers (Momol et al 2004). These CaYMV-specific primers generated the expected 565 bp product, corresponding to the virus polyprotein, from total DNA extracted from symptomatic leaves using a Plant DNeasy Mini Kit (Qiagen, Maryland, USA). No products were amplified from non-symptomatic plants.

PCR amplified products were purified using a Pure link Quick PCR purification kit (Invitrogen by Life Technologies). PCR products were ligated, cloned (pGEM-T Easy Vector System; Promega, USA) and sequenced (UMN-BMGC, USA) to confirm their identity. Raw sequences were edited (Sequencher, Gene Codes Corporation, MI, USA) and deposited in GenBank under accession number KJ890481 (K1) and KJ890482 (K2). Isolate K1 and K2 share 98.6% nucleotide sequence identity and 99.5% amino acid sequence identity (Pearson et al 1997). K1 has 99% nucleotide sequence identity to reported CaYMV polyprotein gene sequences (HE774734.1, KJ890482.1, HE774733.1, and EF189148.1). K2 has 99% nucleotide sequence identity to published CaYMV polyprotein gene sequences (HE774734.1, KJ890481.1, HE774733.1, and EF189148.1)

No virus has been reported in Kenya in cannas, and to our knowledge this is the first report of CaYMV in the country. The nucleotide sequences of the two clones obtained from symptomatic cannas were 99% identical to each other and to the original CaYMV genomic sequence. Based on symptoms, EM, ISEM, PCR, and sequence analysis it is concluded that CaYMV which was previously reported in Japan; the USA; Italy; the Netherlands (Marino et al 2007); and India (Kumari et al 2014) is also present in Kenya. Current management of this virus in cannas includes to destroy plants with typical symptoms and to use only virus-free rhizomes (which can be indexed by PCR) for propagation. Canna growers should note that although the symptoms varied in cannas in two different geographical locations they were both infected with CaYMV. The incidence of CaYMV should also be studied to assess its impact on the production of cannas in Kenya.

Confirmation of First Report of Orchid fleck virus in *Phalaenopsis* Hybrid Orchids in the USA

doi:10.1094/PHP-BR-15-0018.

Orchidaceae family members are diverse and are used for food, cut flowers, and potted plants. In 2013, the United States sold $246 million of potted orchids and $5.6 million of cut flower orchids. Sixteen *Phalaenopsis* hybrid orchids were submitted for pathogen identification in December 2014. New leaves exhibited necrotic flecks with chlorotic rings (Fig. 6 A) or necrotic lesions with leaf reddening (Fig. 6 B). Older leaves on the same plants were either asymptomatic or had large chlorotic spots. Flowers were asymptomatic (Fig. 6 C). Bacterial streaming was not observed under low magnification and very few bacterial colonies on nutrient broth yeast extract medium were isolated from symptomatic tissues. Serological immunostrip testing for *Cymbidium mosaic virus* and *Odontoglossum ringspot virus* were negative (Agdia Inc., Elkhart, IN). *Brevipalpus* sp. mites were observed by dissecting microscopy on several leaves. Transmission electron microscopy (TEM) of symptomatic leaves using partially purified extracts revealed no virus particles. TEM using a rhabdovirus extraction protocol (Doi et al. 1977) confirmed the presence of bacilliform virus particles. One characterized orchid-infecting bacilliform virus is *Orchid fleck virus* (OFV) (Zheng et al. 2013).

Total RNA was extracted (RNeasy Plant Mini Kit, Qiagen, Valencia, CA) and tested by one-step reverse-transcription PCR (RT-PCR) with an OFV specific primer (mN2) and degenerate primer (polydT/SP6) designed to amplify an 800 base pair (bp) portion of the nucleoprotein gene within RNA 1 (Blanchfield et al. 2001). Fifteen out of

sixteen plants tested positive for OFV. All positive reactions resulted in 380-bp, 800-bp, and 882-bp products (Fig. 7).

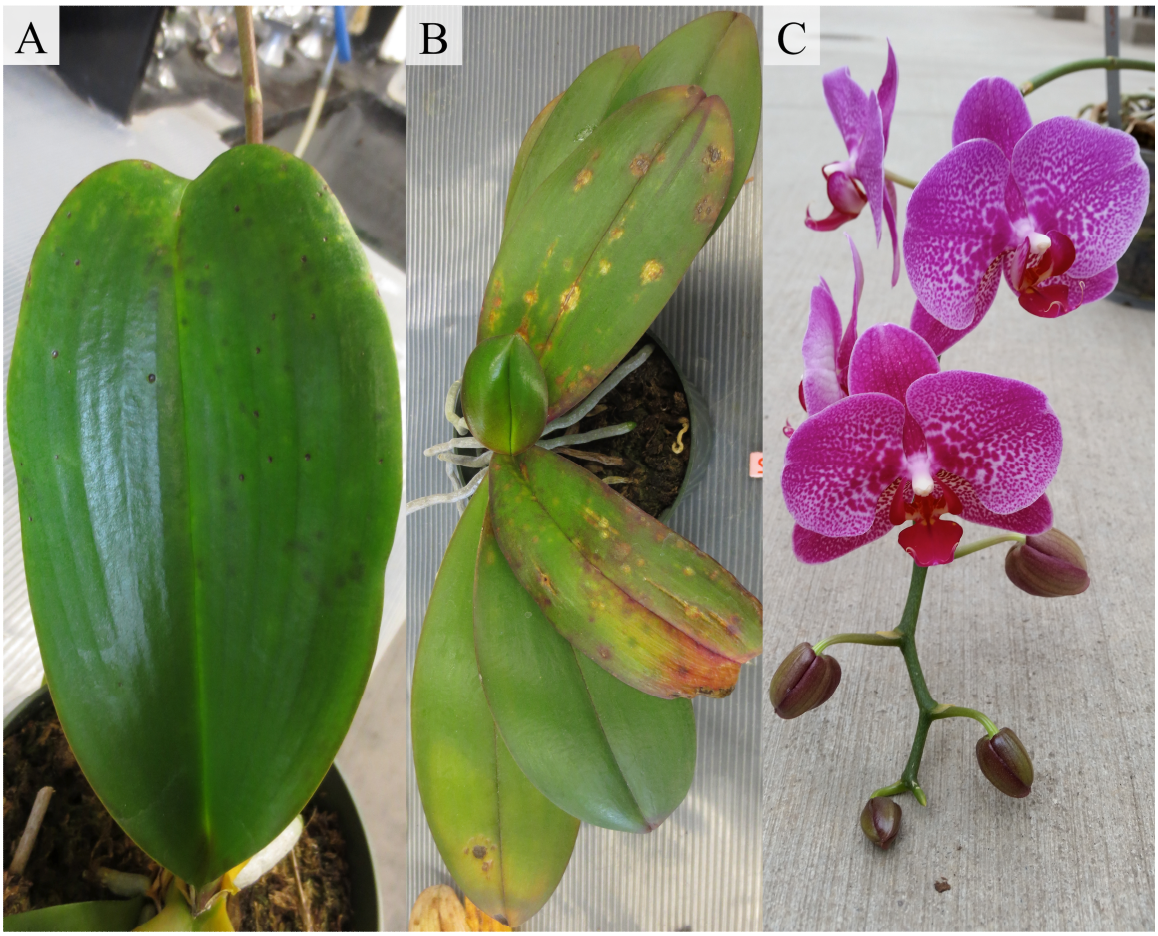

Figure 6. Symptoms of *Phalaenopsis hybrida* orchids infected with *Orchid fleck virus*, submitted in December 2014. The plants were tested by electron microscopy and one-step reverse transcription PCR and were positive for OFV. A. Leaves with necrotic flecks and chlorotic rings. B. Leaves with necrotic lesions and leaf reddening. C. Flowers were asymptomatic.

These three products from two plants were gel-purified (PureLink Quick Gel Extraction Kit; Invitrogen, Waltham, MA), ligated, and cloned (pGEM-T Easy Vector System; Promega, Fitchburg, WI). Two or three clones were sequenced in both directions

(University of Minnesota Genomics Center, Minneapolis, MN) and the consensus sequence (Sequencher 5.1; Gene Codes Corp., Ann Arbor, MI) for the 800-bp product's 660 bp open reading frame was deposited in GenBank (Accession Nos. KR074431 and KR822590). All products were 100% identical to each other. The 660-bp ORF had 100% query cover and 99% sequence identity to reported nucleoprotein genes from OFV isolates in Australia (Accession Nos. AF343871.1, AF321777.1, and AF343872.1), South Africa (AF343874.1), Germany (AF343875.1), and Brazil (AF321776.1). The 380-bp product was identical to the first 380 bases of the 800-bp product. The 882-bp product encoded the forward primer sequence, had 66% identity to *Elaeis guineensis* putative transporter ArsB (XP_010935806.1), and was likely amplified from orchid mRNA.

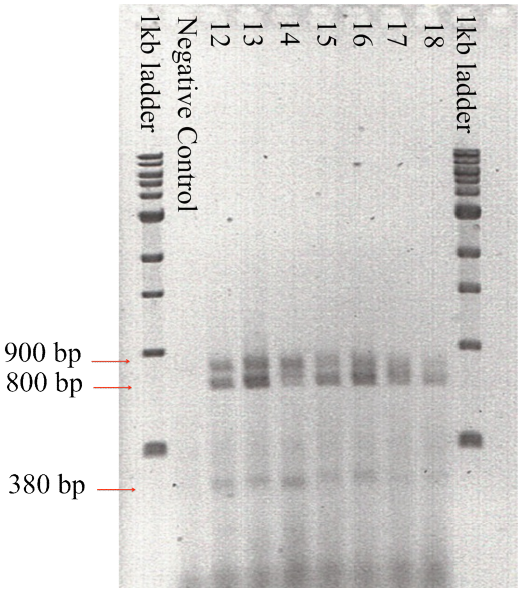

Figure 7. Symptomatic orchids numbered 12 to 18 had total RNA extracted and tested by one-step RT-PCR. The outside lanes contain a 1-kb New England Biolab ladder. The negative control reaction used sterile water. All positive reactions resulted in a 380, 800, and 880 bp product as the red arrows indicate.

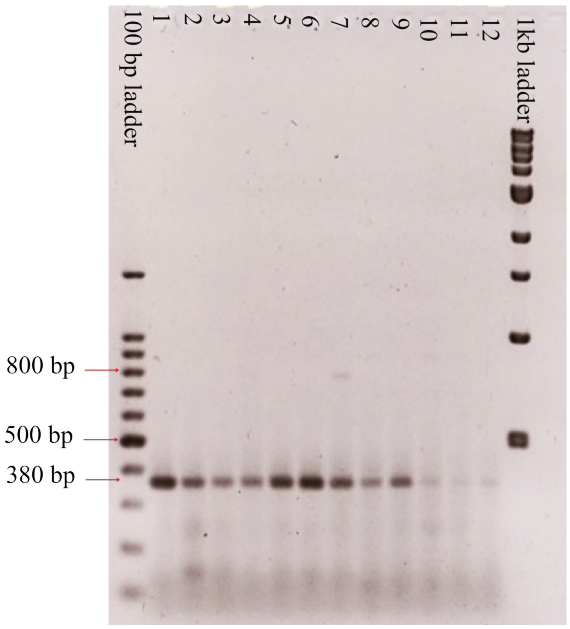

Figure 8. Asymptomatic orchids numbered 1-12 obtained from commercial producers and tested by one-step RT-PCR for the presence of *Orchid Fleck Virus*. The left lane contains a 100 bp ladder. The right lane contains a 1 kb ladder. Eleven reactions (samples 1-6, 8-12) produced a 380 bp product while one reaction produced a 380 bp and the targeted 800 bp product (sample 7).

Twelve asymptomatic *Phalaenopsis* hybrid orchids acquired in February 2015 from commercial growers were tested as described above for the presence of OFV. *Brevipalpus* sp. mite exoskeletons were observed by dissecting microscopy. Eleven reactions yielded a 380-bp product while one reaction had a 380-bp and 800-bp product (Fig. 8). First-strand cDNA was made using the reverse primer (polydT/SP6) and SuperScript III First-Strand Synthesis System (Invitrogen). cDNA was purified using a Pure link Quick PCR purification kit (Invitrogen) and used in a GoTaq (Promega) PCR with the mN2 and polydT/SP6 primer pair. All 12 orchids tested positive for OFV when cDNA was created first (Fig. 9). These results suggest that from these asymptomatic

plants infected with this virus isolate, a one step RT-PCR diagnostic can yield false negatives.

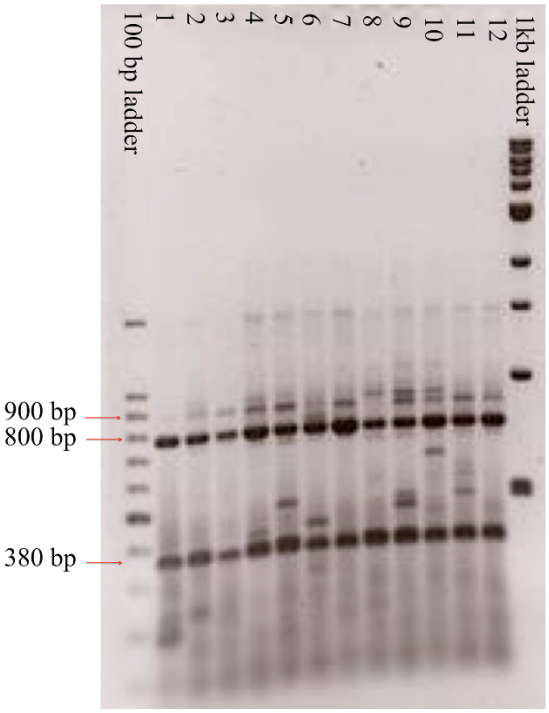

Figure 9. Asymptomatic orchids (1-12) obtained from commercial producers and tested by creating cDNA and then completing a PCR reaction. The left lane contains a 100 bp ladder. The right lane contains a 1 kb ladder. All reactions produced a 380 bp, 800 bp, and 880 bp product, along with other bands likely amplified from plant RNA. These results suggest the one-step RT-PCR reaction with these primers can yield false negatives for this isolate of *Orchid fleck virus* in asymptomatic *Phalaenopsis* hybrid orchids.

A previous report, commonly cited as a United States OFV detection, only describes uncharacterized bacilliform virus-like particles of varying sizes observed by TEM in ultrathin sections of *Brassia* and *Cymbidium* (Ko et al. 1985). This is the first report to confirm OFV infection in the United States by microscopy and sequence analysis. OFV can be spread mechanically (Doi et al. 1977) or by the false spider mites

Brevipalpus californicus and *B. phoenicis* in a persistent manner (Kondo et al. 2003; Hogenhout et al. 2008). It is likely that some, if not all, of the first group of *Phalaenopsis* submitted were infected with OFV at the time of purchase (from commercial growers 3 months to 5 years ago) and was then spread to any non-infected plants in the same location by the false spider mite. OFV has previously been reported in Australia, Brazil, Costa Rica, Denmark, Germany, Japan, and Korea (Blanchfield et al. 2001, Zheng et al. 2013). Current management recommendations include purchasing virus-tested orchids, maintaining sterilization between plants, and testing mother plants prior to tissue culture propagation for the presence of OFV.

Chapter II.

Development of ELISA to detect Orchid Fleck Virus using antibodies produced against *Escherichia coli* expressed matrix protein and phosphoprotein

Abstract

Orchid fleck virus (OFV), a member of the genus *Dichorhavirus* of the family *Rhabdoviridae*, causes necrotic and chlorotic ringspots and fleck symptoms in plants. OFV has been reported in orchids word-wide and in Lilyturf in Australia. A detection method using reverse transcription polymerase chain reaction has been developed but would be expensive to use to screen large numbers of plants and can give false negatives in asymptomatic *Phalaenopsis hybrida* orchids. It is important to develop a reliable, inexpensive method to detect this virus to avoid using infected material for tissue culture propagation and breeding. Therefore, I developed polyclonal antibodies for use in serological detection methods. Polyclonal antibodies were produced in rabbits and prepared against *Escherichia coli* expressed OFV phosphoprotein (P) and matrix protein (M). The resulting antiserums were assayed in PTA-ELISA and DAS-ELISA. OFV P antisera in PTA-ELISA were very specific and readily differentiated between healthy and OFV infected orchid (*Phalaenopsis hybrida*) tissue. OFV M antisera in PTA-ELISA detected only the purified protein they were raised against, and did not differentiate between healthy or OFV infected tissue. IgG was purified from OFV P antiserum and conjugated with alkaline phosphatase. Purified OFV P IgG had a weak reaction against OFV infected tissue in PTA-ELISA. Enzyme conjugated OFV P IgG in DAS-ELISA had

very low detection of OFV infected orchid tissue. The results indicate that OFV P polyclonal antibodies are sensitive, have high efficacy in PTA-ELISA, and could be utilized to rapidly screen large numbers of plants for OFV.

Introduction

Orchids (*Orchidaceae*) are a large and diverse group of flowering plants used for potted plants, cut flowers, and food. Major cultivated orchid species include: *Arachnis, Ascocentrum, Cattleya, Cymbidium, Dendrobium, Laelia, Oncidium, Paphiopedilum, Phalaenopsis, Renanthera, Vanda* and their hybrids (Zettler et al 1990). In 2015 the total USA wholesale value for orchids sold as potted flowering plants was $367.5 million, as the number one selling potted flowering plant, and cut flowers was $8.2 million (USDA Floriculture Crops 2015 summary). Viruses are major pathogens of orchids and can reduce plant vigor and also the number and quality of flowers (Zettler et al 1990). More than 25 viruses have been reported to infect orchids but *Cymbidium mosaic virus* (CymMV) and *Odontoglossum ringspot virus* (ORSV) are the most commonly studied and detected viruses in orchids world-wide (Wong et al 1994; Zettler et al 1987). However, *Orchid fleck virus* (OFV) has also been detected in orchids from different genera from around the world (Blanchfield et al 2001). CymMV and ORSV can be asymptomatic in plants but have effective immunosticks and ELISA kits available for diagnosis. There are currently no commercially available tests for OFV.

OFV infection can cause symptoms of necrotic and chlorotic ringspots, necrotic flecks and lesions, and leaf reddening; but does not cause flower distortion (Alfonso et al

2016; Bratsch et al 2015; Blanchfield et al 2001). OFV has been reported in orchids world-wide and in Lilyturf, *Liriope spicata*, in Australia (Blanchfield et al 2001; Ramos-González et al 2015; Mei et al 2016). OFV can be transmitted mechanically and by the false spider mite, *Brevipalpus californicus* Banks, in a persistent manner from orchid to orchid, bean (*Phaseolus vulgaris* L.), and New Zealand spinach (*Tetragonia expansa* Murr.) (Maeda et al 1998).

OFV is a member of the genus *Dichorhavirus* of the family *Rhabdoviridae* (Alfonso et al 2016). OFV particles are non-enveloped and bacilliform or bullet shaped of 100-150 nm long by 32-40 nm wide, encapsidating a bipartite negative sense single stranded RNA genome (Kondo et al 2006). RNA 1 encodes five proteins while RNA 2 encodes one (Kondo et al 2006). OFV has been observed to associate in the inner membrane of the nuclear envelope and endoplasmic reticulum (Kitajima et al 2001). Due to their relatively large size and association with plant membranes rhabdoviruses require a rhabdovirus specific extraction protocol to visualize particles using transmission electron microscopy (Doi et al 1977). Reverse transcription polymerase chain reaction (RT-PCR) detection of OFV has been developed but can result in false negatives and is expensive to do on a large scale (Blanchfield et al 2001; Bratsch et al 2015).

Polyclonal antibodies against whole viruses or recombinant virus proteins can be made for use in serological detection methods (Hull 2002). Whole virions can be difficult and time consuming to obtain for use in the production of antibodies. Recombinant proteins expressed in prokaryotic systems, like *Escherichia coli* or yeast, are becoming more commonly used as they are relatively easy to produce and available in high

concentrations (Hull 2002; Alkowni et al 2011). The limiting factor for using recombinantly produced virus proteins is available sequence data, so antiserum against plant viruses has traditionally been prepared to purified virus particles. Kondo *et al* (2009) developed polyclonal antiserum against *E. coli* expressed OFV proteins for use in characterizing the structural proteins of OFV viral particles, but this antiserum is not available and there are currently no alternative serological based method to detect OFV.

Typically plant virus coat proteins are used for expression in *E. coli* or yeast cells. However, rhabdovirus particles consist of the genome encapsidated by the nucleocapsid protein, which is surrounded by a host derived phospholipid membrane (Redinbaugh and Hogenhout 2005). The matrix, phospho, and glycoproteins are embedded in the lipid membrane (Redinbaugh and Hogenhout 2005). OFV is an atypical rhabdovirus with nonenveloped particles that resemble the condensed RNP-M core of rhabdovirus virions (Rose and Whitt 2001). These particles contain the genome encapsidated by nucleocapsid proteins surrounded by phosphoprotein, matrix protein, and RNA-dependent RNA polymerase proteins (Kondo et al 2009). Two proteins were chosen for the production of polyclonal antibodies. The matrix protein (M), encoded by RNA 1 ORF 4, and the phosphoprotein (P), encoded by RNA 1 ORF 2 (Kondo et al 2009).

In this study I describe two methods of expressing recombinant *Orchid fleck virus* proteins followed by the production of polyclonal antibodies. The antibodies were validated for detection of OFV using plate trapped antigen (PTA)-ELISA and DAS-ELISA for screening orchids. The objectives of this research were to produce polyclonal

antibodies specific for OFV and develop a serological-based assay for reliable, cost effective, and routine detection of OFV in infected orchids and other plants.

2.0 Materials and Methods

Two OFV proteins were chosen for use in the production of polyclonal antibodies. OFV P (phosphoprotein) coding region was obtained by PCR amplification and cloned into an expression vector while a codon optimized version of OFV M (matrix protein) coding region was synthesized and then cloned into an expression vector.

2.1 Virus source, PCR amplification and cloning [OFV P]

Primers were designed to amplify the entire open reading frame of OFV P from deposited sequences of OFV RNA 1 (AB244417.1, AB516442.1) (Andreas et al 2007). Total RNA was extracted (RNeasy Plant Mini Kit, Qiagen, Valencia CA USA) from OFV infect *Phalaenopsis hybrida* leaf tissue and used to produce cDNA using SuperScriptIII First-Strand Synthesis System (Invitrogen) and primer OFV_P_R2 (5'-TGGAGTCCGGTGAGTCACTA-3'). The cDNA was purified (Pure link Quick PCR purification kit, Invitrogen USA) and used in a GoTaq (Promega) PCR with the primers OFV_P_F2 (5'-CCCTGGATGCCATGAACAGT-3') and OFV_P_R2. The PCR cycle consisted of 95 C for 5 minutes followed by 40 cycles of 95 C for 30 seconds, 57 C for 30 seconds, 72 C for 1 minute with a final extension of 72 C for 10 minutes. The reaction yielded a 980 base pair product. Two products were purified (Pure link Quick PCR purification kit, Invitrogen USA) and sequenced in both directions (UMGC, St Paul USA). The two sequences were 100% identical. The sequences were trimmed to the CDS (Sequencher 5.1, Gene Codes Corp., Ann Arbor MI) and deposited in Genbank.

To facilitate Gateway cloning, the verified cDNA had Att sites added using primers designed to amplify the CDS, OFV_P_F+Att (5'-GGGGACAAGTTTGTACAAAAAAGCAGGCTGGATGTTCACTACCAAGGTAAAT-3') and OFV_P_R+Att (5'-GGGGACCACTTTGTACAAGAAAGCTGGGTGCTAGTCCAGGCATGGCCT-3') in a PrimeSTAR HS DNA Polymerase (TaKaRa Bio USA) reaction using a 3-step PCR cycle which consisted of 98 C for 10 seconds, 55 C for 10 seconds, and 72 C for 1 minute repeated for a total of 30 cycles. The 775 bp product was gel purified (Invitrogen PureLink Quick Gel Extraction Kit) and recombined into the pI-DONR vector (Olszewski unpublished) using BP Clonase II (Invitrogen). The resulting plasmid was propagated in *E. coli* MC1061/P3 (ThermoFisher Scientific). Clones were plated on LB agar with 10 µg/mL tetracycline and 15 µg/mL ampicillin. Viable clones were picked and grown in five mL LB with 10 µg/mL tetracycline and 15 µg/mL ampicillin overnight at 37 C. Plasmids were purified (IBI Scientific High-Speed Plasmid Mini Kit, USA) and digested with EcoRV restriction enzymes for 1 hour at 37 C, and run on a 1.5% agarose gel to identify recombinant clones.

2.2 Virus source, plasmid synthesis OFV M

Deposited OFV M CDS sequences, bases 3830-4381 (AB244417.1, AB516442.1) were analyzed at the nucleotide and amino acid level and the sequences were 99% identical (NCBI Blast). The CDS of codon 4 from the original OFV isolate from *Cymbidium* species in Japan was used for expression in *E. coli* (AB244417.1) (Kondo et al 2006). Codon optimized OFV M flanked by Att sites in the pIDTSMART-AMP

plasmid was purchased (Integrated DNA Technologies USA). Plasmid was amplified for use in experiments by cloning (pGEM-T Easy Vector System, Promega, Fitchburg WI USA) and purified from overnight cultures (Zippy Plasmid Miniprep Kit, Zymo Research USA). Uncut plasmid was recombined into the pI-DONR vector (Olszewski unpublished) using BP Clonase II (Invitrogen) and propagated in *E. coli* MC1061/P3 (ThermoFisher Scientific, USA). Clones were plated on LB agar with 10 μg/mL tetracycline and 15 μg/mL ampicillin. Viable clones were picked and grown in five mL LB with 10 μg/mL tetracycline and 15 μg/mL ampicillin overnight at 37 C. Plasmids were purified (IBI Scientific High-Speed Plasmid Mini Kit, USA), digested with PVUII HF restriction enzymes for 1 hour at 37 C, and run on a 1.5% agarose gel to identify recombinant clones.

2.3 Preparation of recombinant pET32a_OFV plasmids

The coding regions were subcloned by recombination into the expression vector pET32 DEST A using LR Clonase II (Thermo Fisher Scientific, USA). The resulting recombinant plasmids were transformed into *E. coli* MC1061 and transformed cells were selected with 100 μg/mL ampicillin. Ampicillin resistant cells were grown in five mL LB with 100 μg/mL ampicillin and their plasmids were purified (IBI Scientific High-Speed Plasmid Mini Kit, USA) and digested with PvuII (OFV P) or PvuII and EcoRV individually (OFV M) restriction enzymes for 1 hour at 37 C. Digested plasmids were run on 1.5% agarose gels to identify the desired recombinant plasmids which were purified (Zippy Plasmid Miniprep Kit, Zymo Research USA) and sequenced (MCLab, USA) to confirm the clone was correct.

2.4 Protein Expression

Rosetta 2(DE3) Singles Competent Cells (Novagen, EMD Millipore USA) were transformed with the His-tagged recombinant pET32DEST A plasmids. Cells were plated onto LB agar with 75 μg/mL ampicillin and 20 μg/mL chloramphenicol and incubated at 37 C overnight. Viable cells were grown overnight in LB with 75 μg/mL ampicillin and 20 μg/mL chloramphenicol at 37 C.

For expression of the recombinant proteins 500 mL of LB with 75 μg/mL ampicillin and 20 μg/mL chloramphenicol was inoculated with 5 mL of an overnight culture and grown at 37 C and 200 RPM to an optical density (OD_{595}) of 0.5. Isopropyl-beta-D-1-thiogalactopyranoside (IPTG) was then added to a final concentration of 0.3 mM to induce recombinant protein expression. After 2 hours of additional growth at 37 C cells were pelleted. Protein expression was verified by SDS-PAGE (Laemmli, 1970) using a 4-20% TruPAGE separating gel. Electrophoresis was done at 180 V for 30 minutes and gels were stained with Coomassie brilliant blue G-250 stain (Sigma) for 1 hour and destained with 7% acetic acid and 40% methanol for 2 hours.

2.5 Protein Purification

Five hundred mL of induced, pelleted OFV M and P were resuspended with 10 mL lysis buffer and lysed using a french press standard protocol. The samples were clarified by centrifuging at 7000 g at 4 C for 25 minutes. Aliquots (6 μl) were analyzed by SDS-PAGE as in 2.4. Experiments indicated the proteins were insoluble so the protein bodies were analyzed for solubility using varying concentrations of urea. Aliquots were analyzed by SDS-PAGE as described in 2.4.

The remaining induced *E. coli* pellets were processed as above and the protein bodies were solubilized. The solubilized proteins were mixed with four mL equilibrated TALON Metal Affinity Resin and the Batch/Gravity-Flow Column Purification protocol was followed (TaKaRa Bio USA). Fractions were collected and protein concentration was analyzed by standard Bradford microassay protocol (Bradford, 1976; Wright et al 1996). Fractions with the highest concentration had protein size and purity verified by SDS-PAGE as described in 2.4.

2.6 Antibody Production

Purified protein (3 mg) was sent for antibody production in New Zealand White rabbits (Pacific Immunology, USA). Three rabbits were used for each antigen. Rabbits had an initial immunization with purified recombinant protein emulsified with Complete Freund's Adjuvant (day 0, week 1). Following the first immunization rabbits were immunized with purified recombinant protein emulsified with Incomplete Freund's Adjuvant three times for a total of four immunizations over 10 weeks. Serum was collected at week 7, 9, 11, 13. Final bleeds were collected in week 14.

2.7 PTA-ELISA

Plate trapped antigen-enzyme linked immunosorbent assay (PTA-ELISA) was performed according to procedures described by Koenig (1981). Incubation times were modified to 1 hour at 37 C for antigen absorption, 1 hour at room temperature for 5% nonfat dry milk in 1X PBS, 1 hour at 37 C for labeling antibody, 1 hour at 37 C for enzyme conjugated detecting antibody, and 1 hour or more at room temperature for enzyme substrate. Nunc MaxiSorp plates (Apogent); secondary antibody of monoclonal

anti-rabbit IgG-alkaline phosphatase, antibody produced in mouse (Sigma-Aldrich) at 1:2,000 (v/v) dilution in conjugate buffer; and one mg/mL p-nitrophenyl phosphatate (PNPP) (ThermoFisher Scientific) were used for all PTA-ELISA experiments. Absorbance (A_{405}) was read after a period of incubation at room temperature.

Plates were coated with unclarified homogenized healthy or OFV infected *Phalaenopsis hybrida* orchid leaf tissue diluted 1:10 (w/v) in carbonate coating buffer. *P. hybrida* leaf tissue that had tested positive by RT-PCR with bacilliform particles observed by transmission electron microscopy was considered virus infected. Leaf tissue that was considered negative had no particles observed by TEM and tested negative by two-step RT-PCR. The same healthy and virus-infected tissues were used for all experiments using plant tissue.

Differences in the final bleed antibody titers between animals were tested by diluting OFV M and P antiserums 1:1,000 (v/v) in conjugate buffer. Absorbance (A_{405}) was read after 19 and 41.5 hour incubation at room temperature.

OFV M antiserum was diluted 1:1,000 (v/v) in conjugate buffer and tested against purified recombinant OFV M protein at 1.5 ng/mL in carbonate coating buffer. Absorbance (A_{405}) was read after an 18 hour incubation at room temperature.

The optimal plant dilution was tested using OFV P1 antiserum at 1:1,000 (v/v) and plant tissue dilutions of 1:5; 1:10, 1:20, and 1:50 (w/v) in carbonate coating buffer. Absorbance (A_{405}) was read after an 18 hour incubation at room temperature.

Optimal concentration of OFV P primary antibody for use in PTA-ELISA was determined using the most sensitive antiserum previously identified (from animal 1, P1)

diluted 1:1,000; 1:2,000; 1:4,000; 1:8,000; 1:10,000; and 1:20,000 (v/v) in conjugate buffer and tested against healthy and infected plant tissue at a 1:10 (w/v) dilution. Absorbance (A_{405}) was read after a 19 hour incubation at room temperature.

2.8 IgG use in ELISA

IgGs were purified from serum by ammonium sulfate precipitation followed by ion exchange chromatography on DEAE-cellulose (Ball et al 1990). IgG was conjugated to bovine intestine alkaline phosphatase (Mybiosource) using standard protocol (Ball et al 1990). The prepared conjugate was stored at 4 C with 1% (w/v) BSA and 0.02% (w/v) NaN_3.

PTA-ELISA using 1:10 sample dilution and 2 or 5 µg/mL purified OFV P1 IgG was completed to determine the effectiveness of purified IgG. Absorbance (A_{405}) was read after a 19 hour incubation at room temperature.

DAS-ELISA was performed according to procedures described by Clark and Adams (1997). 1 µg/mL OFV P1 rabbit IgG was used for trapping and OFV P1 IgG-AP at 1:1,000 and 1:5,000 (v/v) dilutions in conjugate buffer for detecting the virus. Absorbance (A_{405}) was read after a 20 hour incubation at room temperature.

3.0 Results

Plasmid preparation

Both OFV M and OFV P sequences were identical to original sequences (purchased plasmid or PCR amplified product respectively) used. OVF P coding region was deposited in Genbank under accession number KX932045.

Expression

The purchased OFV M codon optimized coding regions was 552 base pairs encoding 184 amino acids was expressed in the pET32DEST A vector downstream of the polyhistidine tag. PCR amplification using OFV P specific primers yielded an amplicon of 981 base pairs encoding 327 amino acids expressed in the pET32DEST A vector downstream of the polyhistidine tag. SDS-PAGE analysis of total proteins and soluble and insoluble pellet fractions from IPTG-induced *E. coli* cells showed good expression of M (Figure 1) and P (Figure 2) proteins but indicated the proteins were in inclusion bodies. Proteins were solubilized and purified on TALON metal affinity columns. SDS-PAGE shows purity of proteins sent to a private company for antiserum production (Figure 1 and 2).

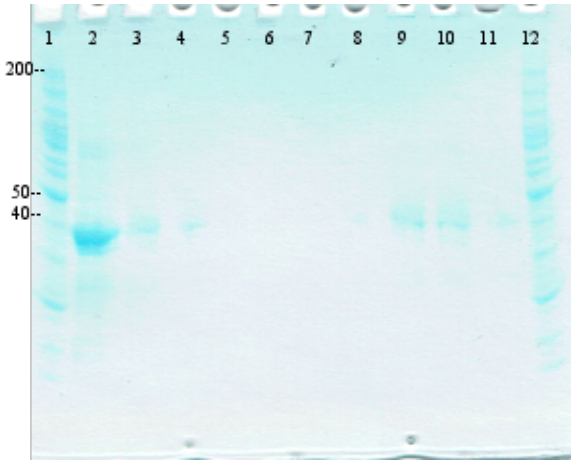

Figure 1. Expressed recombinant OFV matrix protein examined by SDS-PAGE. Lane 1 ThermoFisher PageRuler protein ladder, 200, 50, and 40 kDa marked. Lane 2 insoluble protein bodies from clarified lysate. Lane 3 solubilized clarified lysate. Lane 4 unbound fraction from TALON columns. Lane 5-11 elution fractions from TALON purification columns. Lane 5 fraction 1. Lane 6 fraction 2. Lane 7 fraction 3. Lane 8 fraction 4. Lane 9 fraction 5. Lane 10 fraction 6. Lane 11 fraction 7. Lane 12 protein ladder.

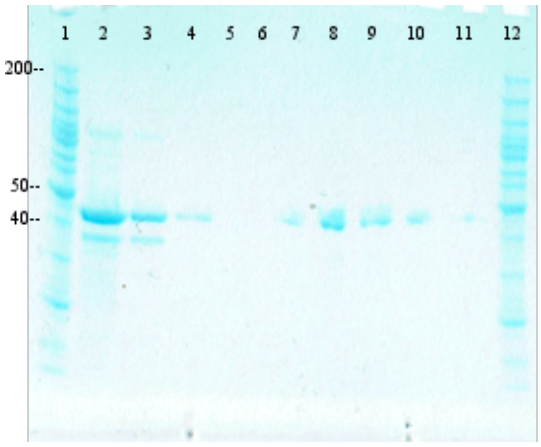

Figure 2. Expressed recombinant OFV phosphoprotein examined by SDS-PAGE. Lane 1 ThermoFisher PageRuler protein ladder, 200, 50, and 40 kDa marked. Lane 2 insoluble protein bodies from clarified lysate. Lane 3 solubilized clarified lysate. Lane 4 unbound fraction from TALON columns. Lane 5-11 elution fractions from TALON purification columns. Lane 5 fraction 1. Lane 6 fraction 3. Lane 7 fraction 5. Lane 8 fraction 6. Lane 9 fraction 7. Lane 10 fraction 8. Lane 11 fraction 9. Lane 12 protein ladder.

PTA-ELISA

Differences in final bleed antibody titers against OFV M and OFV P in three animals per protein were observed and recorded in Table 1 and 2. Antibodies are labeled for animal and protein. OFV M antiserums are labeled M1, M2, and M3 for animal 1, animal 2, and animal 3. OFV P antiserums are labeled P1, P2, and P3 for animal 1, animal 2, and animal 3. OFV M had very low absorbance and there was little difference in the absorbance readings between animals. OFV P antiserums had very strong reactions and the strongest reaction was observed with OFV P1.

OFV M antiserums were tested against purified protein to determine if the antibodies could detect the protein they were raised against. Antiserums were diluted 1:1,000 (v/v) and tested against 1.5 ng/mL purified M protein used as an antigen. Results

are presented in Table 3. OFV M antiserums did react more strongly to purified protein than to infected plant tissue but were not as reactive as OFV P antiserums.

The optimal plant tissue sample dilutions was identified by testing dilutions of 1:5, 1:10, 1:20, and 1:50 (w/v) leaf tissue with OFV P1 antiserum diluted 1:1,000 (v/v). Absorbance readings were taken after 18-hours. Results are presented in Table 4. Highest absorbance readings were recorded with 1:5 and 1:10 (w/v) sample dilutions.

Optimal dilution of P1 antiserum was determined by testing dilutions of 1:1,000; 1:2,000; 1:4,000; 1:8,000; 1:10,000; and 1:20,000 (v/v) against 1:10 (w/v) healthy and virus-infected samples. Results are presented in Table 5. OFV P1 antiserum at 1:4,000 and 1:8,000 gave the strongest and most specific reactions.

Purified OFV P1 IgG was tested by PTA-ELISA to determine if it was effective. Samples were diluted 1:10 (w/v) and 2 and 5 μg/mL IgG was used in PTA-ELISA. Results are presented in Table 6. OFV P1 IgG had low absorbance readings.

OFV M Differences in Animal Antibody Titer Concentration						
	19 hours			41.5 hours		
	H	I	I/H	H	I	I/H
M1	0.007	0.033	4.7	0.090	0.129	1.4
M2	0.032	0.054	1.7	0.156	0.173	1.1
M3	0.024	0.043	1.8	0.121	0.145	1.2
Blank	0			0.03		

Table 1. OFV M animal antibody titer differences in PTA-ELISA were recorded with a 1:10 (w/v) plant leaf tissue sample and 1:1,000 (v/v) antiserum dilution. Absorbance readings (A_{405}) were recorded for animal 1, M1, animal 2, M2, and animal 3, M3 final bleed antiserums at incubation times of 19 and 41.5 hours. H is healthy, virus-free orchid leaf tissue, I is virus-infected leaf tissue, and I/H is the ratio of infected to healthy absorbance values. Readings are the average of 12 wells for both healthy and infected samples per antisera and average of 8 wells for the blank control with only PNPP.

OFV P Differences in Animal Antibody Titer Concentration						
	19 hours			41.5 hours		
	H	I	I/H	H	I	I/H
P1	0.035	3.00	86	0.114	3.00	26
P2	0.017	1.76	103	0.087	3.00	34
P3	0.034	1.65	49	0.114	2.73	24
Blank	0			0.002		

Table 2. OFV P animal antibody titer differences in PTA-ELISA were recorded using a 1:10 (w/v) plant leaf tissue sample and 1:1,000 (v/v) antiserum dilution. Absorbance readings (A_{405}) were recorded for animal 1, P1, animal 2, P2, and animal 3, P3 final bleed antiserums at incubation times of 19 and 41.5 hours. H is healthy, virus-free orchid leaf tissue, I is virus-infected leaf tissue, and I/H is the ration of infected to healthy absorbance values. Readings are the average of 12 wells for both healthy and infected samples per antisera and average of 8 wells for the blank control with only PNPP.

Detection of Recombinant Protein by OFV M Antisera			
Blank	M1	M2	M3
0	0.865	1.201	0.748

Table 3. OFV matrix antisera used in PTA-ELISA to detect 1.5 ng/mL purified recombinant OFV M protein. Absorbance readings (A_{405}) were recorded after 18-hours. Readings are the average of 16 wells for each antisera from three different animals and 8 wells for the blank control with only PNPP.

Optimal Plant Sample Dilution			
	H	I	I/H
1:5	0.04	2.17	54
1:10	0.04	1.61	40
1:20	0.045	1.32	29
1:50	0	0	0
Blank	0		

Table 4. PTA-ELISA optimization of orchid leaf tissue dilution. H is healthy, virus-free orchid leaf tissue, I is virus-infected leaf tissue, and I/H is the ratio of infected to healthy absorbance values. Absorbance readings (A_{405}) were recorded after a 18 hours. Readings are the average of 12 wells for each antisera and 8 wells for the blank control with only PNPP.

Optimal P1 Antiserum Dilution			
	19 hours		
	H	I	I/H
Blank	0		
1 to 1,000	0.024	2.874	120
1 to 2,000	0.003	1.741	605
1 to 4,000	0.001	1.052	1052
1 to 8,000	0.0004	0.545	1454
1 to 10,000	0.000	0.508	*508
1 to 20,000	0.008	0.245	31

Table 5. Various dilutions of OFV P1 antiserum against 1:10 (w/v) orchid leaf tissue to determine optimal working concentration for use in PTA-ELISA. H is healthy, virus-free orchid leaf tissue, I is virus-infected leaf tissue, and I/H is the ratio of infected to healthy absorbance values. Absorbance readings (A_{405}) were recorded after 19-hours. Readings are the average of 8 wells for dilutions from 1:1,000-1:10,000 and for the blank control with only PNPP. The 1:20,000 dilution readings are the average of 4 wells. * The 1:10,000 I/H ratio was determined using 0.001 for a healthy absorbance value as the value using 0 cannot be calculated.

OFV P1 IgG PTA-ELISA			
	19 hours		
	H	I	I/H
Blank	0		
2 ug/mL	0	0.05	*50
5 ug/mL	0.0157	0.174	11

Table 6. PTA-ELISA using 1:10 (w/v) orchid leaf tissue and 2 or 5 µg/mL purified OFV P1 IgG. H is healthy, virus-free orchid leaf tissue, I is virus-infected leaf tissue, and I/H is the ratio of infected to healthy absorbance values. Absorbance readings (A_{405}) were recorded after 19-hours. Readings are the average of 20 wells for the antisera and 8 wells for the blank containing only PNPP. * The 2 µg/mL I/H ratio was determined using 0.001 for a healthy absorbance value as the value using 0 cannot be calculated.

DAS-ELISA

Purified OFV P1 IgG at 1 µg/mL was used for trapping and enzyme conjugated IgG at 1:1,000 and 1:5,000 (v/v) dilution were tested in DAS-ELISA. Absorbance readings were taken after 20 hours incubation. Results are presented in Table 7.

OFV P1 DAS ELISA			
	H	I	I/H
Blank	0.003		
1:1,000 conjugate	0.0279	0.0211	0.76
1:5,000 conjugate	0.0023	0.0067	3.00

Table 7. DAS-ELISA using plates coated with 1 µg/mL purified OFV P1 IgG, 1:10 (w/v) orchid plant tissue, and 1:1,000 or 1:5,000 (v/v) enzyme conjugated OFV P1 IgG for detection. H is healthy, virus-free orchid leaf tissue, V is virus-infected leaf tissue, and I/H is the ratio of infected to healthy absorbance values. Absorbance readings (A_{405}) were recorded after 20-hour room temperature incubation with PNPP. Readings are the average of 20 wells for the antisera and 8 wells for the blank containing only PNPP.

Discussion

OFV is a mite and mechanically transmissible plant virus originally reported in orchids, but has also been found in Lilyturf and experimentally inoculated into bean (*Phaseolus vulgaris* L.) and New Zealand spinach (*Tetragonia expansa* Murr.) (Maeda et al 1998). Unlike CymMV and ORSV, which have serological tests available for use by commercial producers and hobbyists, there are no commercially available RT-PCR or serological assays for OFV. The globalization of the horticultural plant production process means plants can be exposed to a wider variety of viruses. Without a reliable, inexpensive, and accurate test viruses cannot be identified in new hosts, large conservation collections, breeding programs, or plants destined for tissue culture propagation.

Recombinant OFV proteins were expressed in *E. coli* and purified for use as antigens in polyclonal antibody production. This method was chosen due to difficulties in purifying large quantities of rhabdoviruses from plant tissue and length of time required for *in planta* propagation of virus.

OFV M antisera were much less reactive when tested against infected plant tissue than OFV M antisera (Table 1). OFV M antiserum reacted more strongly when tested against purified recombinant protein (Table 3). The final bleed antisera for OFV M may have a lower antibody titer than the final bleed antisera for OFV P. Antisera collected earlier could be tested to identify any prior weeks with higher antibody titers. The lower reactivity of OFV M antisera may also be due to a very low concentration of free, unassembled, viral matrix protein in OFV infected plant cells. Alternatively, the matrix

protein may not have antigenic epitopes exposed when assembled into mature virus particles. The antiserum does react with purified expressed protein so it could be used for Western Blotting experiments. Future experiments could use sonication to disrupt the plant cells to a greater degree than is accomplished with crushing the tissue to determine if it can be used for diagnostic purposes.

OFV P antiserum reacted very specifically with insignificant background detected when tested (Table 2). OFV P3 had the lowest absorbance readings so it is likely the antibody titer peaked prior to the final bleed. Earlier bleeds could be tested to determine if there is a higher antibody titer comparable to the final bleeds of P1 and P2. OFV P1 reacted the fastest and the most strongly with an acceptable rate of non-specific binding so it was utilized for following experiments. There was a very low amount of absorbance observed for all OFVP antisera after 1 hour of incubation at room temperature (data not shown), but after 19 hours there was very strong absorbance for virus infected tissue. Absorbance values at 41.5 hours of incubation were still very strong for virus infected tissue but the amount of non-specific binding observed with virus-free tissue was much higher than in shorter incubation periods. In general PTA-ELISA experiments using P1 antiserum should be read after an overnight incubation and no longer than a 24-hour incubation.

OFV P1 was tested in PTA-ELISA against various dilutions of plant tissue to determine the best concentration to use in large scale screening experiments (Table 4). Orchid leaf tissue dilutions of 1:5 and 1:10 (w/v) reacted the strongest and had the lowest non-specific binding and should be utilized for future tests.

A wide range of antiserum dilutions were tested to determine the most effective concentration for use in diagnostics (Table 5). After 19 hours a 1:1,000 (v/v) dilution had the strongest absorbance for virus-infected tissue. There was an acceptable amount of absorbance for virus-infected tissue with minimal non-specific binding up to the 1:8,000 (v/v) dilution. Larger dilutions up to 1:20,000 (v/v) did have good levels of absorbance and minimal non-specific binding but would not be recommended for large screening operations due to the weaker reactions observed in comparison with lower dilutions. The best I/H ratio was shown by the 1:4,000 and 1:8,000 (v/v) antisera dilutions. The optimal working concentration of OFV P1 antiserum was determined to be 1:4,000 or 1:8,000 (v/v).

PTA ELISA using purified IgG showed an inhibited reaction compared to whole antiserum (Table 6). A high-titer rabbit antiserum has roughly 5 mg/mL of IgG so the 2 µg/mL and 5 µg/mL concentrations of purified IgG used would correlate to whole antiserum dilutions of 1:2,500 (v/v) and 1:1,000 (v/v) respectively. At those concentrations absorbance readings higher than 1.0 were expected but the purified IgG had readings of only 0.048 and 0.174 respectively.

In DAS-ELISA purified OFV P1 IgG conjugated to bovine intestine alkaline phosphatase did not react strongly against infected tissue (Table 7). In general, antibodies react to their antigens with relatively weak, short range forces that only occur when there is steric compatibility between the antigen and antibody (Mandel 1971). There could be an incompatible reaction between the spatial distribution of the purified IgG and viral epitopes. OFV is a relatively large plant virus (100-150 nm x 32-40 nm) (Kondo et al

2006) and it is possible that the virus particles are not strongly bound to the coating IgG and are rinsing off of the plate prior to the addition of the conjugated IgG. Higher concentrations of coating IgG could be incubated for longer time to see if there is an improved reaction caused by low numbers of available epitopes for IgG to bind. There is limited structural data about the mature OFV particles so conjugated IgG may not be able to reach the antigenic viral epitopes. Decreased sensitivity in DAS-ELISA has previously been attributed to alterations in the detecting IgG steric hindrance caused by the conjugation to alkaline phosphatase enzyme (Hu et al. 1991; Van Regenmortel & Burckard, 1980) and is likely to be a factor reducing the reaction observed in this experiment. The conjugated antibody is reacting with available epitopes but the interacting forces may be too low to withstand the physical forces encountered during rinsing. Divalent antibody fragments (F(ab')2 fragments) of IgG could be used for detecting trapped viral proteins to determine if the conjugated antibody is sterically inhibited (Barbara & Clark 1982).

The minimal background observed with PTA-ELISA indicates the expressed recombinant plant rhabdovirus proteins were suitable for the production of sensitive and specific OFV P polyclonal antiserum. The antiserum can now be used for large scale screening of orchid collections, breeding stock, and plants destined for clonal propagation to limit the spread of this virus. This is important because the virus can be asymptomatic, has a predicted wide host range, and has a variety of symptoms that can develop depending upon species infected.

Chapter III.

Molecular and biological characterization of a new *Nepovirus* causing a leaf mottling disease in *Petunia hybrida*

Abstract

This report describes the complete genome sequence and molecular diagnostics of petunia chlorotic mottle virus (PCMoV), a proposed new member of the genus *Nepovirus.* Icosahedral virus-like particles were isolated from *Petunia hybrida* cuttings with symptoms of interveinal chlorotic mottling. The virus was readily mechanically transmitted with crude sap extracts to healthy *Petunia hybrida*. The virus contains a bipartite RNA genome of 7.6 and 3.8 kb that was sequenced by next generation sequencing combined with 5' RACE amplification and reverse transcription PCR using poly-A tail and virus specific primers. Phylogenetic analysis of the coding regions identified a close relationship to Subgroup A nepoviruses. Based on its particle morphology, sufficiently dissimilar amino acid sequences to known members of the genus *Nepovirus,* conserved motifs, and phylogenetic analysis, PCMoV appears to be a distinct new member of this genus.

Introduction

Petunia hybrida, commonly called the garden petunia, is the most popular annual bedding plant worldwide valued for their prolific, large, and colorful flowers (Bombarely et al 2016). The wholesale value in 2015 of petunia plants exceeded $135 million in the USA alone (2015 USDA Floriculture Crops Summary). Petunias are also used as a

genetic model (van der Krol et al 2016). Petunias belong to the family *Solanaceae* and wild species are natively found in South America from Argentina to Uruguay, Southern Brazil, and the foothills of the Andes (Wijsman 1982). In the early 1800's petunias were imported to Europe and crosses between the wild *P. axillaris* and *P. inflata* were completed resulting in the colorful *P. hybrida* (Wijsman 1982). *P. hybrida* are predominantly propagated by vegetative cuttings and when infected by viruses the virus will persist, being transmitted from infected parent plant to cutting, until measures are taken to propagate from virus-free material (Lesemann 1996). There is a low industry and consumer tolerance for viral symptoms in petunias (Lesemann 1996).

Several pathogens are commonly found in petunias including bacteria, fungi, oomycetes, and viruses. *Ralstonia solanacearum* (formerly *Pseudomonas solanacearum*) and *Acidovorax* spp. can cause bacterial leaf spots and wilt on petunia (Arlat et al; Allen et al 2005; Jones et al 2003). Major fungal diseases include root rot caused by *Rhizoctonia solani*, wilt caused by *Fusarium oxysporum*., and grey mold caused by *Botrytis cinerea* (Daughtrey & Benson 2005, Pataky 1988, Farr et al 1989). Late blight caused by *Phytophthora infestans* causes sunken lesions and stem girdling or crown rot, which can lead to plant death (Deahl & Fravel 2003). Major viral pathogens including *Potato virus Y* (PVY), *Tobacco mosaic virus* (TMV), *Impatiens necrotic spot virus* (INSV), *Tomato mosaic virus* (ToMV), *Alfalfa mosaic virus* (AMV), *Tomato ringspot virus* (ToRSV), *Tobacco streak virus* (TSV), *Cucumber mosaic virus* (CMV), *Petunia vein clearing virus* (PVCV), and *Broad bean wilt virus* 1 (BBWV1) have been found in single and mixed infections causing symptoms of mosaic, chlorosis, necrosis, leaf

deformation, stunting, flower color breaking and vein clearing (Lesemann 1996, Sanchez-Cuevas & Nameth 2002).

In early 2012 *Petunia hybrida* cuttings were obtained with virus-like symptoms derived from plants originally vegetatively propagated in South America. The infected plants had symptoms of interveinal chlorotic mottling on their leaves. The symptoms were distinct from the previously reported viruses infecting petunia. In order to determine the disease causing organism, partially purified extracts were examined by transmission electron microscopy (TEM) and numerous non-enveloped icosahedral virus-like particles were present. No other virus-like particles were observed. To determine the causal pathogen virus-like particles were purified and their nucleic acid was analyzed. Healthy plants were mechanically inoculated with sap from infected leaf tissue. The genome of purified particles was sequenced and a molecular diagnostic test was created. Phylogenetic analysis of the genomic sequences indicated the virus is a new member of the genus *Nepovirus*.

Methods

Virus source and transmission

Virus infected *Petunia hybrida* cuttings were rooted and propagated. Cuttings were allowed to root under a mist bench and removed when roots had fully developed. Healthy *Petunia hybrida* were obtained and examined by transmission electron microscopy to verify their virus-free status. Silicon carbide dusted healthy *P. hybrida* leaves were mechanically inoculated with crude sap extracts from infected *P. hybrida*

leaves in 100 mM phosphate buffer, pH 7.4, containing 0.5% (v/v) 2-mercaptoethanol. Four healthy plants were inoculated. Inoculated plants and virus containing propagated rooted cuttings were kept in a greenhouse at 24 C with 16/8 hrs day/night photoperiod. Greenhouse temperature and relative humidity was logged by Onset HOBO Temperature/Relative Humidity data loggers (Onset Computer Corporation, USA). Inoculated plants were observed weekly for the development of symptoms after which they were examined by transmission electron microscopy (TEM) for the presence of virus-like particles.

Transmission electron microscopy

Symptomatic leaf or flower tissue was partially purified as previously described (Ahlawat et al 1996). Partially purified extracts were examined by TEM after negative staining with 2% (w/v) sodium phosphotungstate (PTA), pH 7.0, containing bacitracin at 100 µg/ml. Average diameter of virus particles was calculated by measuring 50 particles.

Virion purification

Virions were purified from infected *P. hybrida* leaf tissue by differential centrifugation and isopycnic density-gradient centrifugation on Cs_2SO_4 as previously described (Currier & Lockhart 1996).

Nucleic acid extraction and digestion

Guanidinium thiocyanate-phenol-chloroform extraction of total particle-associated nucleic acid was done as previously described from purified virion particles (Chomczynski & Sacchi 1987, Lockhart 1990). Nucleic acid digests were performed with

DNase I (New England BioLabs), RNase A (ThermoFisher Scientific, USA), and mung bean nuclease (New England BioLabs) as previously described (Lockhart 1990).

Next Generation Sequencing

Clonally propagated plants were used as a source for RNA extraction. Total RNA was extracted from symptomatic leaf tissue using a Qiagen RNeasy kit. The RNA was sent to Macrogen (Seoul, Korea) for cDNA library preparation and sequencing as pair-end 100 bp reads on an Illumina HiSeq 2500 system. Sequences were assembled into contigs using CLC Genomics Workbench v 5 (Qiagen). BLASTN and BLASTX queries to NCBI GenBank were used to detect virus-related contigs. To verify virus-like sequences overlapping primer pairs were designed from the putative RNAs and RT-PCR was carried out using illustra Ready-to-Go RT-PCR beads (GE Healthcare).

All RT-PCR products were cloned using pGEM-T Easy Vector System (Promega) and a minimum of three clones per reaction were sequenced in both directions. Sequences were initially assembled in Genious v. 8 but final mapping of the reads to each of the RNAs were performed using CLC Genomics Workbench.

5' end sequencing

The 5' ends of RNA1 and RNA2 were sequenced using 5' RACE System for Rapid Amplification of cDNA ends, version 2.0 (ThermoFisher Scientific). Sequence specific primers used included: RNA1GSP1 (GGTAATTGCGCCCATCATAGTA), RNA2GSP1 (GAACCTCAGACATGGGAACAA), RNA1GSP2 (GGACCAACCTCAACAACTACA), and RNA2GSP2 (CCGGCAGGATACACATTCATTA).

The PCR cycle for dC-tailed cDNA consisted of 94 C for 2 minutes followed by 35 cycles of 94 C for 1 minute, 55 C for 30 seconds, 72 C for 1 minute followed by a final extension of 72 C for 7 minutes. Ten µl of 5' RACE products were analyzed by agarose gel electrophoresis.

After SNAP purification of cDNA a PCR cycle was completed using the kit provided UAP and the RNA1 and RNA2 GSP2 primers. The PCR cycle consisted of: 35 cycles of 94 C for 1 minute; 63 C for 30 seconds; 72 C for 2 minutes followed by a final extension of 72 C for 10 minutes.

Following PCR amplification the products were run on a 0.9% gel. The products were gel purified (Invitrogen PureLink Quick Gel Extraction Kit, Thermo Fisher Scientific USA) ligated, and cloned (pGEM-T Easy Vector Systems, Promega USA). Six clones for each RNA1 and RNA2 were sequenced in both directions (MC Lab, USA). Sequences were assembled using Sequencher 5.1 (Gene Codes Corp., Ann Arbor, MI).

3' end sequencing

The 3' ends were obtained using purified RNA in a SSIII cDNA protocol (Thermo Fisher Scientific) using a primer specific for the poly-A tail, VdTGCR ($v(T)_{14}$GCCCGGGCGGCCGCG). The cycle consisted of 55 C for 90 minutes followed by 70 C for 15 minutes. The cDNA was purified using PureLink PCR Purification Kit (ThermoFisher Scientific, USA). The purified products were used in a GoTaq (Promega) PCR cycle using primer GCR (GCCCGGGCGGCCGCG) and sequence specific primers RNA1For1 (GGCCCGAATGTGCTATTCTA) or RNA2For1 (CTGGAGTAACAGCACCAGATAC). The cycle consisted of 95 C for 5 minutes

followed by 30 cycles of 94 C for 30 seconds, 57 C for 30 seconds, and 72 C for 2 minutes with a final extension of 72 C for 10 minutes.

Phylogenetic analysis

Multiple sequence alignment was performed by ClustalW (Larkin et al 2007) and deposited members of the virus subfamily *Comovirinae* and genus *Nepovirus* (Genbank). The genetic relationship of the viruses was examined using the maximum-likelihood (ML) algorithm by MEGA7: Molecular Evolutionary Genetic Analysis version 7.0 (Kumar, Stecher, & Tamura 2015). For this analysis 1,000 puzzling steps were calculated using the JTT matrix-based model (Jones et al 1992).

Virus Detection

Primers for use in reverse-transcription PCR were designed and tested for use in diagnostic clinics. One primer pair for each RNA1 and RNA2 was developed. Primers to detect RNA 1 are PCMoV_RNA1_F (ACACCACTTCACGGTCATCC) and PCMoV_RNA1_R (CGTCTATCTCCGGCTGTGTC). Primers to detect RNA 2 are PCMoV_RNA2_F (TATCCCGTCCTGACACAGGT) and PCMoV _RNA2_R (GTGAGAGCACCTCGTGGAAA). Total RNA was extracted from healthy (without virus particles) and infected petunia leaves using an RNeasy Plant Mini Kit (Qiagen, USA). A RT-PCR reaction using illustra Ready-To-Go RT-PCR Beads (GE Healthcare Life Sciences, USA), one µl RNasin (Promega, USA), 10 mM primers, and one µl total RNA was completed. The RT-PCR cycle consisted of: 42 C for 45 minutes, 94 C for 5 minutes followed by 35 cycles of 94 C for one minute, 57 C for 45 seconds, 72 C for 45 seconds and a final extension of 72 C for 10 minutes.

Results and Discussion

Virus-like disease symptoms were observed on *Petunia hybrida* unrooted cuttings that originated from South America in 2012. The symptoms consisted of interveinal chlorotic leaf mottling that varied in intensity (Figure 1). The symptoms were not similar to viruses previously reported to infect petunia.

Partially purified extracts from symptomatic petunia tissue were observed by TEM and numerous icosahedral virus-like particles were observed (Figure 2). The particles had an average diameter of approximately 28 nanometers. Both empty and intact virus particles were observed in extracts from symptomatic petunia tissue while there were no particles observed in extracts from healthy petunia plants.

The virus was readily transmitted by sap inoculation from infected petunia leaves to healthy petunias. Disease symptoms similar to those observed in the host plant appeared in all inoculated plants 3-4 weeks post-inoculation. TEM analysis showed the previously virus-free healthy plants were infected with icosahedral virus-like particles after symptoms developed. The virus was later identified by RT-PCR thus confirming the etiology of the disease. Symptoms were reduced in severity during the summer months when greenhouse temperatures were between 32-38 C during the day and between 22-28 C at night.

Figure 1. Interveinal chlorotic mottling symptoms observed in *Petunia hybrida*. A: Left, healthy petunia leaf. Middle and right infected petunia leaves with symptoms. B: Symptoms observed in infected petunia cuttings.

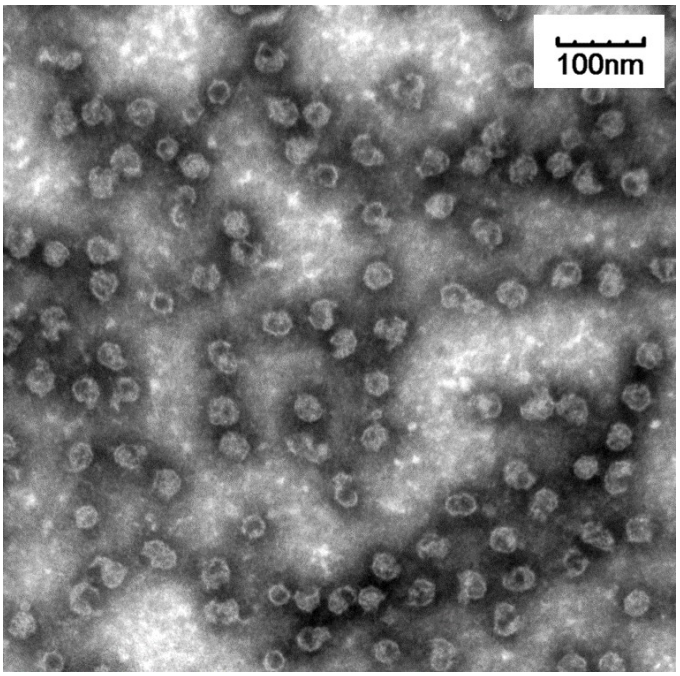

Figure 2. Partially purified symptomatic tissue extracts stained with 2% phosphotungstic acid and observed by transmission electron microscopy at 66,000X magnification. Scale bar is 100 nanometers. Numerous icosahedral empty and intact virus like particles are present in symptomatic tissue.

Nucleic acids extracted from purified virus-like particles were completely digested by RNase A (ThermoFisher Scientific, USA) and mung bean nuclease (New England BioLabs), but not DNase I (New England BioLabs) treatment indicating they are composed of a single-stranded RNA genome. Nucleic acids loaded on an agarose gel revealed two species (RNA1 and RNA2) of approximately 8,000 and 4,000 nucleotides (nts) in length, respectively.

The complete nucleotide sequences of RNA1 and RNA2 were determined. Over 33 million raw reads were obtained from the RNA Seq petunia cDNA library. These reads assembled into 332,696 contigs. A subset of 10,877 contigs longer than 500 nts were analyzed by BLAST algorithms. Two of the contigs showed similarity to virus members of the genus *Nepovirus* by BLAST analysis. 5,097,509 of 33,236,858 reads were mapped to 7,542 nt RNA1 contig with an average of 66,937X coverage per nt position. Similarly, 3,909,142 reads mapped to 3,716 nt RNA2 contig with an average of 102,773X coverage per nt position.

The majority of the RNA sequence was determined using next-generation sequencing. The 5' and 3' ends were determined using a 5' RACE kit and virus specific primers with primers specific for the poly-A tail.

RNA 1 is 7,615 nucleotides (nts) excluding the poly A tail. RNA 1 encodes a single open reading frame (ORF) that starts at the 5' AUG (nt 115 to 118) and terminates at UAG (nt 7062 to 7065). The 5' and 3' untranslated regions are 114 and 565 nts respectively. A BLASTP analysis of polyprotein 1 showed a close relationship to subgroup A nepoviruses (Table 1).

Analysis of the predicted amino acid sequence of RNA1 revealed conserved amino acid motifs characteristic of the RNA dependent RNA polymerase (RdRp), helicase, viral genome-linked protein, and cysteine protease of subgroup A nepoviruses. The polyprotein 1 encoded by RNA1 contains consensus motifs I through VIII, conserved in the RdRp of positive-strand RNA viruses (Koonin et al 1993). This ORF also contains the characteristic motifs for the Hel domain of picorna-like viruses belonging to the helicase superfamily III, characterized by the presence of the motif "A", followed by motif "B", and motif "C" (Gorbalenya et al 1990). In addition, polyprotein 1 contains the triad of conserved residues in the cysteine protease (C-Pro) region of positive-strand RNA viruses (Gorbalenya et al 1989). The deduced polyprotein of RNA 1 has a leucine, amino acid 1417, in the substrate binding pocket of protease as previously described for nepoviruses in subgroup A or B (Margis & Pinck 1992). The viral genome-linked protein (VPg) is predicted to be present between the HEL and C-Pro domains, by comparison with nepoviruses. The conserved *Nepovirus* and *Comovirus* VPg consensus sequence predicted by Mayoa and Fritsch was present (Mayoa & Fritsch 1994).

RNA 2 is 3,804 nts excluding the poly-A tail. RNA 2 encodes a single ORF that starts at the 5' AUG (nt 119-121) and terminates at UAG (nt 3,476 to 3,478). The 5' and 3' untranslated regions are 118 and 326 nts respectively. A BLASTP analysis of the polyprotein 2 showed close relationship to nepoviruses of subgroup A (Table 1).

The cleavage site for polyprotein 2 between the movement protein and coat protein was predicted to be V/A based on sequence analogy with nepoviruses. The coat protein (CP) is predicted to start at amino acid 852 and end at 1371 containing the

conserved *Nepovirus* CP motif FYGR in the C-terminus with a substitution from R to the charged amino acid D, as is observed with *Tobacco ringspot virus* (Koonin et al 1993). The ORF also contains the LPL motif in the putative MP domain (Koonin et al 1991).

Nepoviruses in subgroup A and B have a 3' UTR less than 1 kb in length for both RNA 1 and 2 while subgroup C has long 3' UTR of approximately 1.4 kb. The 3' UTR of RNA1 of this virus is 550 nts long while RNA2 has a 326 nts long UTR. The particle morphology, genome organization and relatedness to nepoviruses, and conserved motifs indicate the new virus is a member of the genus *Nepovirus*, subgroup A.

Direct comparisons between the Petunia chlorotic mottle virus polyprotein 1, polyprotein 2, the Pro-Pol region of polyprotein 1 between the Pro main motif "CG" and Pol motif VI "GDD" (Le Gall et al 2008), and the coat protein (CP) regions of this virus and other nepoviruses of subgroup A, B, and C were completed (Table 1). All regions had relatively low percentages of identity as is typically observed for the *Nepovirus* family.

Multiple sequence alignments for polyprotein 1 and polyprotein 2 were generated using ClustalW and the ML method was used for phylogenetic analysis. The resulting alignments were bootstrapped 1,000 times to assess the tree topology (Saitou & Nei, 1987). Polyprotein 1 of petunia chlorotic mottle virus shows close similarity to *Nepovirus* subgroup A (Figure 3A). Polyprotein 2 aligns with a member of subgroup C, however there are only 2 members of subgroup C with completed polyprotein 2 sequences (Figure 3B). That node was weakly supported with a bootstrap value of 74%.

Table 1

Virus	Polyprotein 1	Polyprotein 2	Pro-Pol	CP
Subgroup A				
ArMV	35	25	50	25
GFLV	34	23	51	23
RpRSV	27	22	43	22
TRSV	33	24	44	23
Subgroup B				
BRSV	32	24	45	22
CNSV	32	22	45	19
GCMV	32	24	47	24
TBRV	32	24	47	23
Subgroup C				
BRV	32	25	46	25
ToRSV	30	22	41	22

Table 1. Percentage of amino acid similarity between the amino acid sequences of the Petunia chlorotic mottle virus polyprotein 1, polyprotein 2, Pro-Pol region (Le Gall et al 2008), and predicted coat protein (CP) of this virus to the same regions of other respective members of the genus *Nepovirus*. Name abbreviations and accession numbers follow: ArMV= *Arabis mosaic virus* (YP_053925.1, AAK07728.1), GFLV=*Grapevine fan leaf virus* (NP_619689.1, AAK07727.1), RpRSV= *Raspberry ringspot virus* (AAQ73822.1, AAQ73823.1), TRSV= *Tobacco ringspot virus* (AAQ73822.1, NP_919039.1), BRSV= *Beet ringspot virus* (NP_620112.1, NP_620113.1), CNSV= *Cycas necrotic stunt virus* (NP_620619.1, NP_620620.2), GCMV=*Grapevine chrome mosaic virus* (NP_619705.1, NP_619704.1), TBRV= *Tomato black ring virus* (NP_958814.1, NP_758518.1), BRV=*Black currant reversion virus* (NP_612604.1, NP_612586.1), ToRSV= *Tomato ringspot virus* (NP_620765.1, NP_620762.1).

The genus *Nepovirus*, of the sub-family *Comovirinae*, of the family *Secoviridae* has a high level of genomic diversity between genus members (King 2011). To determine if petunia chlorotic mottle virus is more closely related to other members of the

Comovirinae sub-family phylogenetic trees were constructed with representative members from that family (Figure 4). Polyprotein 1 showed close relationship with members of the genus *Nepovirus*, subgroup A (Figure 4 A). The bootstrapping value associated with the petunia chlorotic mottle virus and *Arabis mosaic virus* node was 99% while the entire subgroup A node was 51%. Polyprotein 2 also showed close relationship with members of the genus *Nepovirus* in subgroup A (Figure 4 B) with a bootstrap value of 100 for the subgroup A cluster node.

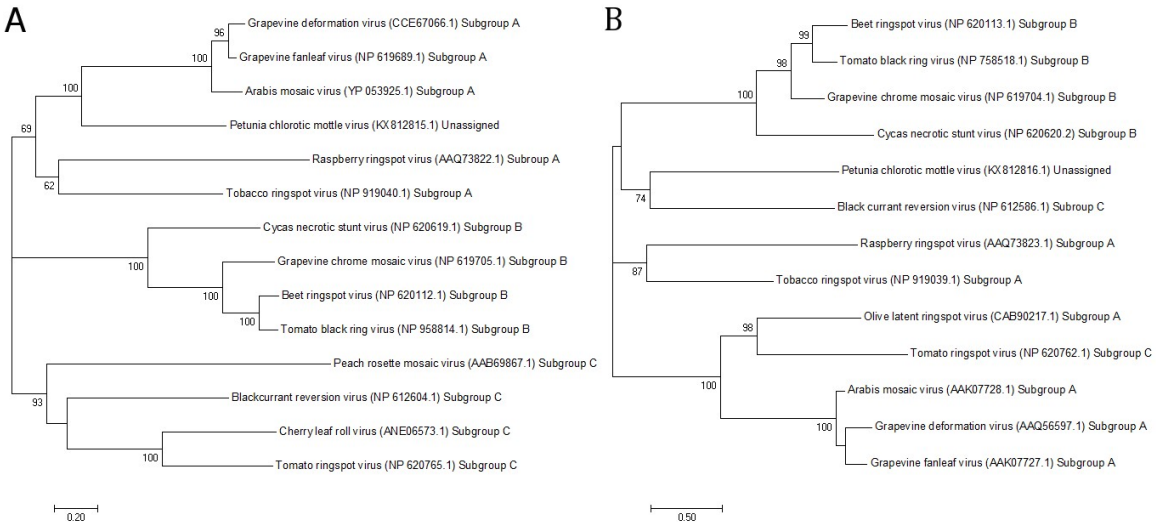

Figure 3. Phylogenetic analysis of Petunia chlorotic mottle virus and selected members of the genus *Nepovirus* based on: A. Polyprotein 1; B. Polyprotein 2. Phylogenetic trees were constructed using the maximum likelihood algorithm. The numerical values represent bootstrap (1000 replicates) values above 50. The scale bars correspond to substitutions per amino acid site. The accession numbers of the amino acid sequences and *Nepovirus* subgroup (A-C) used for analysis are listed with each virus name.

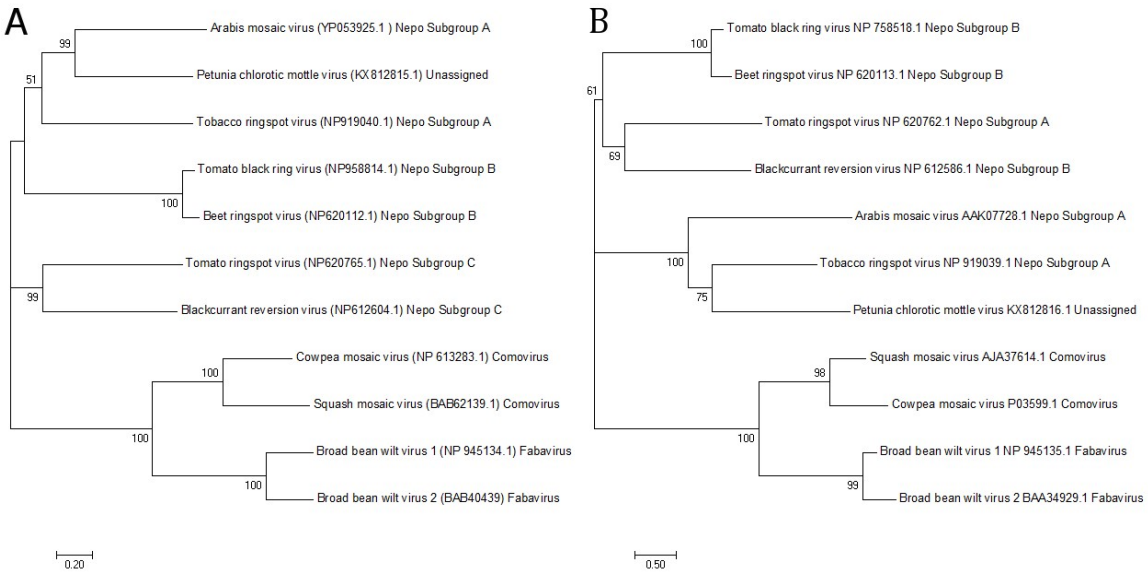

Figure 4. Phylogenetic analysis of Petunia chlorotic mottle virus and selected members of the sub-family *Comovirus* based on: A. Polyprotein 1; B. Polyprotein 2. Phylogenetic trees were constructed using the maximum likelihood algorithm. The numerical values represent bootstrap (1000 replicates) values above 50. The scale bars correspond to substitutions per amino acid site. The accession numbers of the amino acid sequences used for analysis are listed with each virus name.

A molecular diagnostic assay was created for use with this virus. Both pairs of primers worked well and gave a strong reaction for virus infected tissue but did not react with healthy tissue. More isolates from different plant and country origins will need to be tested to further validate these primers.

The particle morphology, genome organization, conserved motifs, and phylogenetic relationship indicate this virus is a new member of the genus *Nepovirus*, subgroup A. I propose the name Petunia chlorotic mottle virus (PCMoV) for this new *Nepovirus*.

Chapter IV.

Characterization of proteinaceous filaments associated with disease-like symptoms in the *Asteraceae* plant family

Abstract

This project arose from Lockhart laboratory observations that filamentous protein structures are associated with leaf and flower deformation in several species in the plant family *Asteraceae*. These filamentous structures are similar in morphology to filamentous viruses or animal and fungal prions. Conserved proteins of different sizes are associated with filaments from sunflower, gerbera, zinnia, and chrysanthemum. Protein sequencing data indicates the filaments are an aggregate of a plant protease inhibitor belonging to the kunitz soybean trypsin inhibitor (KTI) family. Western blotting using antibodies prepared against sunflower KTI label the proteins associated with purified filaments. These data provide strong evidence that the fibrils are mainly composed of a plant KTI. Future experiments could elucidate if they share similarity to described amyloid, prion, or conformational disease-like protein aggregates or if they are a novel class of insoluble proteinaceous aggregates.

Introduction

High levels of filamentous virus-like structures were associated with disease-like leaf and flower deformation symptoms in various species in the family *Asteraceae* including: chrysanthemum and pyrethrum (*Chrysanthemum* spp.), gerbera (*Gerbera jamesonii, G. hybrida*), sunflower (*Helianthus annuus*), and zinnia (*Zinnia hybrida*).

The *Asteraceae* or *Compositae* family is one of the largest families of flowering plants belonging to the *Angiospermae* group. The *Asteraceae* group name comes from the type genus *Aster,* Greek for star, and is referring to the star-like flowers of the family. There are more than 23,000 species in this family and it is rivaled in size by only the *Orchidaceae* family. The *Asteraceae* family is found throughout the world in all habitats except Antarctica and the extreme Arctic (Kadereit & Jeffrey 2007). Economically important members include: sunflower, *Helianthus annuus*, used for trans-fat free oil and a whole seed crop; pyrethrum, *Chrysanthemum cinearіifolium* and *C. coccineum*, from which the natural insecticide pyrethrin is extracted; stevia, *Stevia rebaudiana*, a low calorie sweetener; lettuce, *Lactuca sativa*, a leafy vegetable; Jerusalem artichoke or sunchoke, *H. tuberosus*, a tuberous root vegetable; and others (Kadereit & Jeffrey 2007; Casida 1980; Brandle et al 1998). Numerous genera are used horticulturally for cut flowers or ornamental plants like the chrysanthemum, *Chrysanthemum* spp.; gerbera daisy, *Gerbera* spp.; coneflower, *Echinaceae* spp.; dahlia, *Dahlia* spp.; pot marigold, *Calendula offinalis*; aster, *Aster* spp.; zinnia, *Zinnia* spp.; sunflower, *Helianthus* spp.; and many others (Kadereit & Jeffrey 2007).

Numerous pathogens are commonly found causing disease in this group of plants. Diseases of sunflower, *Helianthus annuus* L., include bacterial diseases including: apical chlorosis, *Pseudomonas syringae*; bacterial leaf spot, *Pseudomonas* spp.; bacterial wilt, *Pseudonomas solanacearum*; crown gall, *Agrobacterium tumefaciens;* and erwinia stalk and head rot, *Erwinia carotovora*. Fungal diseases include: alternaria leaf blight, *Alternaria* spp.; botrytis head rot (gray mold), *Botrytis cinereal*; charcoal rot,

Macrophomina phaseolina; downy mildew, *Plasmopara* spp.; fusarium stalk rot, *Fusarium* spp.; phoma black stem, *Phoma* spp.; powdery mildew, *Erysiphe* spp., *Leveillula* spp., *Sphaerotheca fuliginea*; pythium seedling blight and root rot, *Pythium* spp.; rhizoctonia seedling blight, *Rhizoctonia solani*; rhizopus head rot, *Rhizopus spp.*; rust, *Puccinia* spp., *Uromyces junci*; sclerotinia rot and wilt, *Sclerotinia* spp.; septoria leaf spot, *Septoria helianthi* Ellis & Kellerm; and verticillium wilt, *Verticillium* spp. Nematode pathogens include the American dagger, *Xiphinema americanum* Cobb; pin, *Paratylenchus projectus* Jenkins; lesion, *Pratylenchus* spp.; reniform, *Rotylenchulus* spp.; root knot, *Meloidogyne* spp.; spiral, *Helicotylenchus* spp.; and stunt, *Tylenchorhynchus nudus* and *Quinisulcius acutus*. Viruses including *Cucumber mosaic virus, Tobacco streak virus,* and *Tobacco mosaic virus* are also observed in sunflowers (Gulya & Masirevic, 1993, Bhat et al 2002).

This project arose from observations that disease like flower and leaf deformation symptoms were associated with high levels of filamentous virus-like particles. The filamentous particles were found to not contain a virus-like genome and instead are composed of one major plant protein. The protein was identified as a plant protease inhibitor belonging to the soybean kunitz trypsin inhibitor family.

Methods

Transmission Electron Microscopy

Symptomatic leaf tissue was partially purified as previously described (Ahlawat et al 1996). Partially purified extracts were examined by TEM after negative staining with

2% (w/v) sodium phosphotungstate (PTA), pH 7.0, containing bacitracin at 100 μg/ml. Average diameter of filaments was calculated by measuring 50 particles.

Particle purification

Particles were purified from symptomatic chrysanthemum (*Chrysanthemum* spp.), gerbera (*Gerbera jamesonii, G. hybrida*), sunflower (*Helianthus annuus*), or zinnia (*Zinnia hybrida*) leaf tissue by differential centrifugation and isopycnic density-gradient centrifugation on Cs_2SO_4 as previously described (Currier & Lockhart 1996).

Nucleic acid extraction

Guanidinium thiocyanate-phenol-chloroform extraction of total particle-associated nucleic acid was done as previously described from purified virion particles (Chomczynski & Sacchi 1987, Lockhart 1990).

Enzyme digests

Nucleic acid digests were performed with DNase I (New England BioLabs), RNase A (ThermoFisher Scientific, USA), and mung bean nuclease (New England BioLabs) as previously described (Lockhart 1990). TurboDNase was also used according to manufacturer's standard protocol (Thermo Fisher Scientific).

SDS-PAGE

Purified filaments were subjected to SDS-PAGE (Laemmli, 1970) using a 4-20% TruPAGE separating gel (Sigma-Aldrich, USA). Electrophoresis was completed at 150 V for 10 minutes followed by 180 V for 30 minutes. Gels were stained with Coomassie brilliant blue G-250 stain (Sigma) for 1 hour and destained with 7% acetic acid and 40% methanol for 2 hours. Gels were stored in 7% acetic acid.

N-terminal protein sequencing

N-terminal protein sequencing was completed by the Protein Facility of the Iowa State University Office of Biotechnology. Purified samples, as verified by TEM and previous SDS-PAGE gels, were submitted for analysis. Proteins were separated on Laemmli polyacrylamide gels (Laemmli, 1970). Proteins were transferred to polyvinylidene difluoride membrane (PVDF). The membrane was stained with Coomassie brilliant blue R-250: 40% methanol: 10% acetic acid for 5 minutes and destained. Detectable protein bands were excised for sequencing. Samples were sequenced by Edman Degradation using a Perkin Elmer 494 Procise Protein/Peptide Sequencer with an on-line 140C PTH Amino Acid Analyzer (Applied Biosystems, Inc).

Antibody Production

Primers were designed to amplify the entire open reading frame of the sunflower kunitz soybean trypsin inhibitor (KTI). Total DNA was extracted (DNeasy Plant Mini Kit, Qiagen, Valencia CA USA) from sunflower leaf tissue and used in a GoTaq (Promega) PCR with the primers Helianthus_KTI_F (5'- ACCACCACTGCCGACGTTA -3') and Helianthus_KTI _R (5' - CTACTCAGATTGAACA - 3'). The PCR cycle consisted of 95 C for 5 minutes followed by 35 cycles of 95 C for 30 seconds, 60 C for 30 seconds, 72 C for 1 minute with a final extension of 72 C for 10 minutes. The reaction yielded a 612 base pair product. Two products were purified (Pure link Quick PCR purification kit, Invitrogen USA) and sequenced in both directions (UMGC, St Paul USA). Sequences were assembled into contigs (Sequencher 5.1, Gene Codes Corp., Ann

Arbor MI). The two sequences were 100% identical. The sequence was deposited in GenBank (KY039997).

The verified cDNA had Att sites added using primers designed to amplify the CDS, AttKTI_F (5'-GGGGACAAGTTTGTACAAAAAAGCAGGCTGGACCACCACTGCCGACGTTA-3') and AttKTI_R (5'-GGGGACCACTTTGTACAAGAAAGCTGGGTGCTACTCAGATTGAACAGAAGC-3') in a PrimeSTAR HS DNA Polymerase (TaKaRa Bio USA) reaction using a three-step PCR cycle which consisted of 98 C for 10 seconds, 55 C for 10 seconds, and 72 C for 1 minute repeated for a total of 30 cycles. The product was gel purified (Invitrogen PureLink Quick Gel Extraction Kit) and recombined into the pI-DONR vector (Olszewski unpublished) using BP Clonase II (Invitrogen). The resulting plasmid was propagated in *E. coli* MC1061/P3 (ThermoFisher Scientific). Clones were plated on LB agar with 10 μg/mL tetracycline and 15 μg/mL ampicillin. Viable clones were chosen and grown in five mL LB with 10 μg/mL tetracycline and 15 μg/mL ampicillin overnight at 37 C. Plasmids were purified (IBI Scientific High-Speed Plasmid Mini Kit, USA) and digested with EcoRV restriction enzymes for one hour at 37 C, and run on a 1.5% agarose gel to identify recombinant clones.

The SF KTI coding region was subcloned by recombination into the expression vector pET32 DEST A using LR Clonase II (Thermo Fisher Scientific, USA). The resulting recombinant plasmids were transformed into *E. coli* MC1061 and transformed cells were selected with 100 μg/mL ampicillin. Ampicillin resistant cells were grown in

five mL LB with 100 μg/mL ampicillin and their plasmids were purified (IBI Scientific High-Speed Plasmid Mini Kit, USA) and digested with EcoRV restriction enzymes for one hour at 37 C. Digested plasmids were run on 1.5% agarose gels to identify the desired recombinant plasmids which were purified (Zippy Plasmid Miniprep Kit, Zymo Research USA).

Rosetta 2(DE3) Singles Competent Cells (Novagen, EMD Millipore USA) were transformed with the His-tagged recombinant pET32DEST A plasmids. Cells were plated onto LB agar with 75 μg/mL ampicillin and 20 μg/mL chloramphenicol and incubated at 37 C overnight. Viable cells were grown overnight in LB with 75 μg/mL ampicillin and 20 μg/mL chloramphenicol at 37 C.

Expression of the recombinant proteins was induced in 500 mL of LB with 75 μg/mL ampicillin and 20 μg/mL chloramphenicol. It had been inoculated with five mL of an overnight culture and grown at 37 C and 200 RPM to an optical density (OD_{595}) of 0.5. Protein expression was induced by the addition of isopropyl-beta-D-1-thiogalactopyranoside (IPTG) to a final concentration of 0.3 mM. After 2 hours of additional growth at 37 C cells were pelleted. Protein expression was verified by SDS-PAGE (Laemmli, 1970).

Five hundred mL of induced, pelleted recombinant protein was resuspended with 10 mL lysis buffer and lysed by a French press following a standard protocol. The samples were clarified by centrifuging at 7000 g at 4 C for 25 minutes. Aliquots were analyzed by SDS-PAGE. The protein bodies were solubilized and mixed with five mL equilibrated TALON Metal Affinity Resin and the Batch/Gravity-Flow Column

Purification protocol was followed (TaKaRa Bio USA). Fractions were collected and protein concentration was analyzed by standard Bradford microassay protocol (Bradford, 1976; Wright et al 1996). Fractions with the highest concentration had protein size and purity verified by SDS-PAGE.

Purified protein (2.5 mg) was sent for antibody production in New Zealand White rabbits (Pacific Immunology, USA). Two rabbits were used. Rabbits had an initial immunization with purified recombinant protein emulsified with TiterMax Gold Adjuvant (Sigma-Aldrich) (day 0, week 1). Following the first immunization rabbits were immunized with purified recombinant protein emulsified with Incomplete Freund's Adjuvant three times for a total of 4 immunizations over 10 weeks. Serum was collected at week 7, 9, 11, and 13. Final bleeds were collected in week 14.

Western blot

Following SDS-PAGE, purified sunflower fibrils were analyzed by Western Blotting as previously described (Burnette 1981). The protocol was modified in the blocking step by using 2% Tween 20 for two minutes as described in Bjerrum et al (1987). A primary antibody of anti-SF KTI final bleed antiserum at 1:1,000 (v/v) dilution and secondary antibody of monoclonal anti-rabbit IgG-alkaline phosphatase, antibody produced in mouse (Sigma-Aldrich) at 1:10,000 (v/v) dilution were used. Alkaline phosphatase was used at a concentration of 0.15 mg/mL (SIGMA*FAST* BCIP/NBT, Sigma-Aldrich, USA).

CID MS/MS sequencing

Purified sunflower fibrils were denatured and analyzed by SDS-PAGE as previously described. The gel was stained with Imperial Protein Stain (ThermoFisher Scientific) and submitted to the Center for Mass Spectrometry & Proteomics (CMSP) Facility (University of Minnesota) for peptide sequence by mass spectrometry. Protein bands of interest were excised to prepare for sequencing and destained (Drbal et al 2001). Proteolytic digestion was completed on the excised protein bands by in-gel trypsin digest using a protocol adapted from Shevchenko et al (1996). The samples were then desalted by STop And Go Extraction (STAGE) TIPS desalting procedure (Rappsilber & Mann, 2003). Mass spectrometry (MS) was completed as described in Lin-Moshier et al (2013).

Peaks Studio 6.0 build 20120620 (Bioinformatics Solutions Inc.) software package was used for interpretation of tandem MS and protein inference (Ma et al 2003). Search parameters included UniProt database (Campanula genera taxonomy ID 91882, accessed Jan 6 2016) concatenated with the common lab contaminants (cRAP) database (http://www.thegpm.org/crap/) and the translated KTI coding region obtained by PCR. In addition an artificial proteome was created by taking the sunflower transcriptome assembled by Trinity (https://www.sunflowergenome.org/transcriptome.html) and translating it using the program ORF (https://github.com/panicbit/orf). This artificial proteome was also used in the search parameters. The remaining search parameters for Peaks were followed as described in Dahlin et al (2015).

Prion prediction programs

The translated SF KTI coding region was examined using the computer algorithms PrionW (Zambrano et al 2015) and PLAAC (Lancaster et al 2014) to evaluate if it shared any identity with prion-like amyloidgenic regions. A computer algorithm for predicting aggregation prone regions in unfolded polypeptide chains, Tango (Fernandez-Escamilla et al 2004), was also used to analyze the translated KTI coding region for sequence similarity to beta sheet, beta turn, alpha helix, beta aggregation, and helix aggregation conserved sequences.

Results

Symptomatic tissue (Figure 1), both leaf and flower petals, contained numerous filamentous structures 7-10 nanometers wide by 20 to greater than 4000 nanometers long (Figure 2).

No nucleic acid was encapsidated in particles purified by cesium-sucrose gradients and subjected to enzyme digests from gerbera daisy (Figure 3) or sunflower (not pictured).

SDS-PAGE of fibrils purified from sunflower, gerbera, and zinnia identified a major protein that migrates with a molecular mass of around 22 kDa and other proteins (Figure 4) that vary between species and preparations.

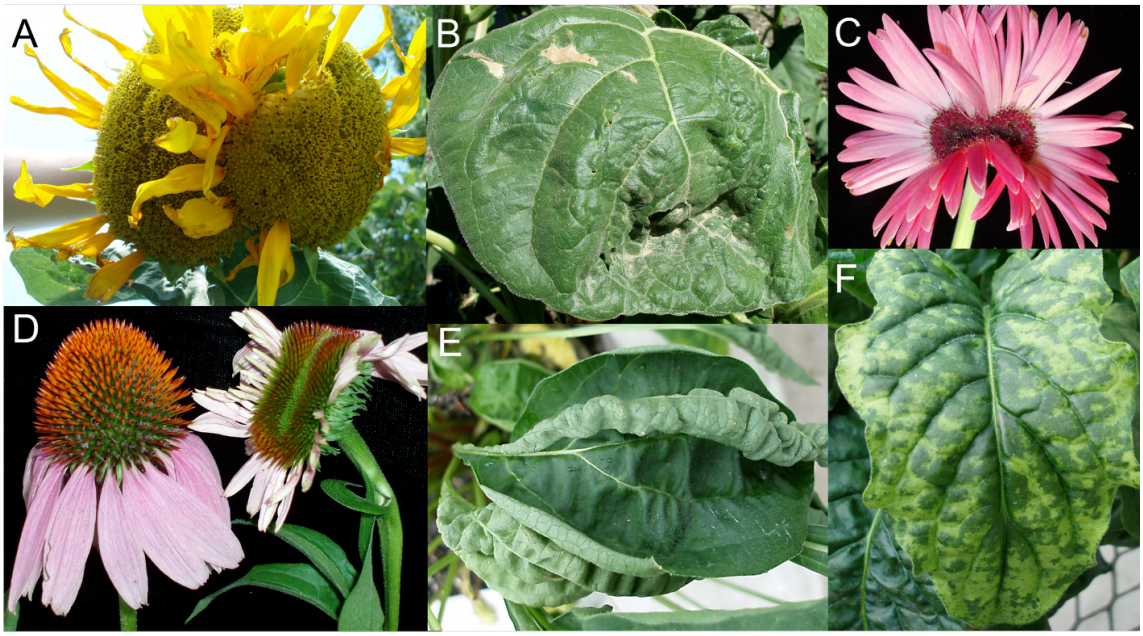

Figure 1. Flower and leaf deformation symptoms associated with high levels of filaments in various members of the *Asteraceae* family. A-B: Sunflower, *Helianthus annuus*, flower doubling (A) and leaf deformation (B); C+F: Gerbera (*Gerbera hybrida*) flower doubling (C) and chlorotic leaf mottling (F); D+E: Coneflower (*Echinacea purpurea*) D: normal flower left, distorted flower right and leaf deformation (E).

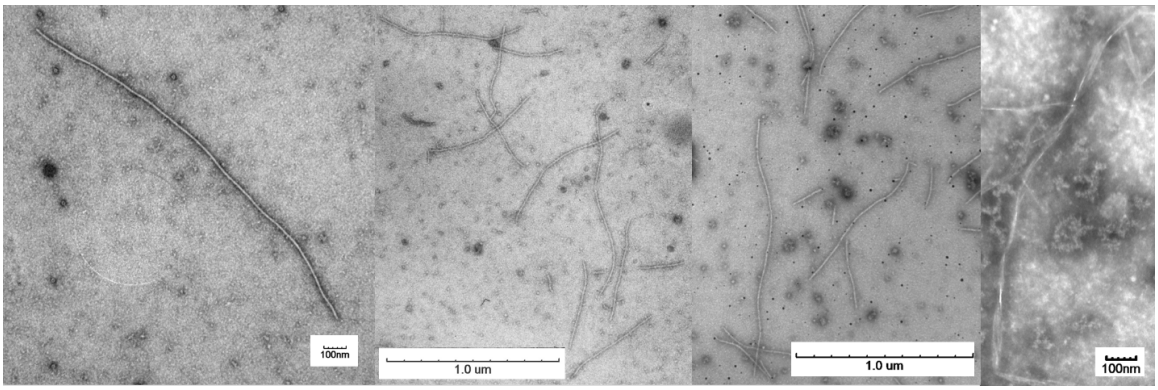

Figure 2. Filaments visualized by transmission electron microscopy from partially purified tissue extracts from sunflower (53,000X), coneflower (31,000X), gerbera daisy (25,000X), and sunflower (53,000X), respectively stained with 2% phosphotungstic acid.

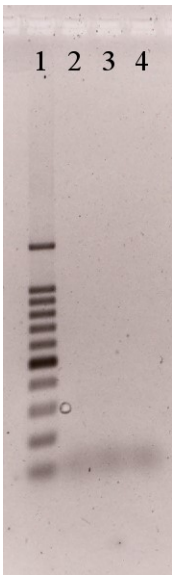

Figure 3. Cesium sucrose gradient purified filaments were treated with TURBO DNase and RNase to eliminate non-encapsidated host nucleic acids, extracted, and combined with proteinase K. Lane 1: 100 base pair ladder, lanes 2-4 varied concentrations of nuclease treated gerbera daisy filament nucleic acid.

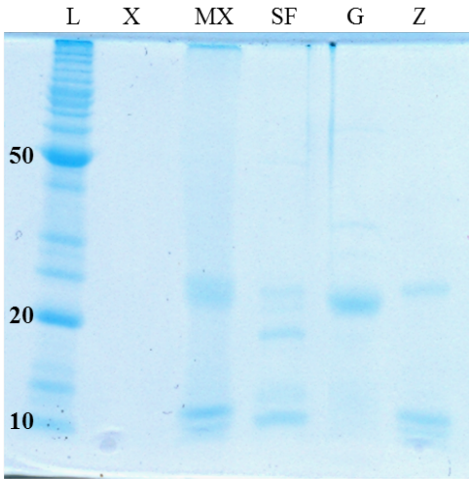

Figure 4. Filaments purified by cesium sucrose gradients were examined by SDS-PAGE. L= ladder, X= blank well, MX=mix of tissue from gerbera and zinnia, SF=sunflower, G= gerbera, Z= zinnia.

N-terminal protein sequencing by Edman degradation was performed on the ~12 and 20 kDa chrysanthemum; ~22 kDa gerbera; and ~12, ~20, and ~55 kDa zinnia proteins associated with purified filaments. The sequences of all of the proteins were nearly-identical (Table 1). A BLAST search of EST sequences revealed that the N-terminal sequences had perfect, or nearly perfect, identity with predicted mature kunitz soybean trypsin protease inhibitors from chrysanthemum (Figure 5).

	Chrysanthemum	Gerbera	Zinnia
12 kDa	ADVIYD(S/S')AGNKLL		ADVIYD(S/S')AGNKL
22 kDa	ADVIYD(S/S')AGNKLL	(S/S')DVIYDSDGNKLLSGVP	ADVIYD(S/S')AGNKL
55 kDa			ADVIYD(S/S')AGNKL

Table 1. N-terminal protein sequencing results for the proteins observed by SDS-PAGE from purified filaments.

```
        1 ADVIYDSVGN KLLKGVPYYI MPLLRGTGGG LTLTRATKDA
Gerbera   SDVIYDSAGN KLLSGVP
 Zinnia   ADVIYDSAGN KL
    Mum   ADVIYDSAGN KLL
Sunflower ADVIYDSAGN K                GTGGG LTLTRA

       41 CPLDVTQEPF ELSYGVPFTI TPIIFDENYV REAYPVSIEA
Sunflower                                 EAYPVSIEA

       81 NVADPCQGSK ILKLSTSDNI VAATATTTKT ITIGGQLNAP
Sunflower NVADPCQGSK

      121 ESCFQLVEDD MMPGLRSYQI QLCPFKCGSN TSTSTDMTCY
Sunflower                 SYQI QLCPFK

      161 NIGLVSDPDG KRFLAPTDAI YPVVFQNSFG SSVASVQSE*
```

Figure 5. Gerbera, zinnia, and chrysanthemum (Mum) N-terminal peptide sequences aligned with predicted translated sunflower kunitz-trypsin inhibitor obtained by PCR (KY039997). Sunflower CID MS/MS protein sequencing results presented in green.

To provide further confirmation that the abundant proteins associated with the fibril proteins are a kunitz soybean trypsin protease inhibitor, the complete coding region of the sunflower KTI with the highest identity to the proteins was cloned and sequenced. The 350 base pair product encodes a protein with sequences that closely matched the N-terminal protein sequences. At the nucleotide level it shared 100% coverage and 93% identity to *Helianthus serpentine* cDNA clones in the EST database (EE636664.1, EE640031.1, EL512083.1). The predicted translation product had high identity with Trypsin and protease inhibitor (Kunitz_legume pfam00197), Soybean trypsin inhibitor (Kunitz) family (STI cd00178), and Soybean trypsin inhibitor (Kunitz) family (STI smart00452).

Sunflower fibril proteins were resolved by SDS-PAGE and the four proteins that were visible (from ~28-55 kDa) (Figure 6) were cut out of the gel, digested with trypsin, and sequences of the resulting peptides were obtained by collision-induced dissociation tandem mass spectrometry (CID MS/MS) analysis. The sequence of four of the trypsin fragments, that were present in each of the protein bands, had 100% identity with predicted fragments from the cloned sunflower KTI (Figure 5).

The coding region was recombinantly expressed in *E. coli,* purified, and used for antibody production. A western blot using the antibodies prepared against the sequenced sunflower KTI labeled the ~11, ~28, ~30, and ~50 kDa proteins from purified sunflower fibrils (Figure 7).

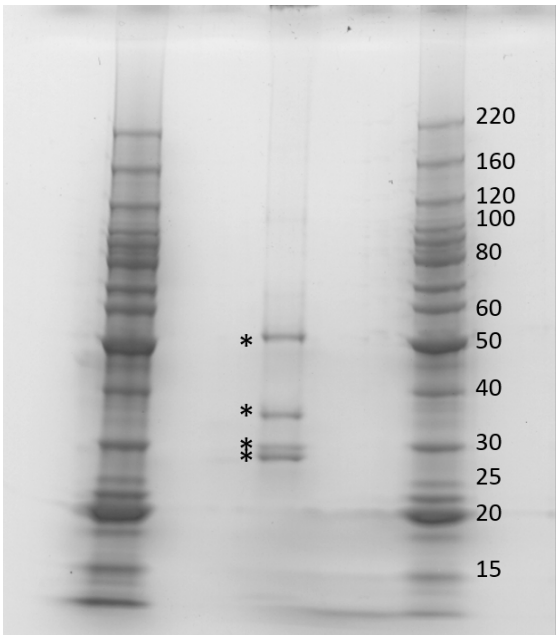

Figure 6. Imperial protein stain of purified sunflower fibrils used for CID MS/MS protein sequencing. Proteins that were sequenced are marked (*).

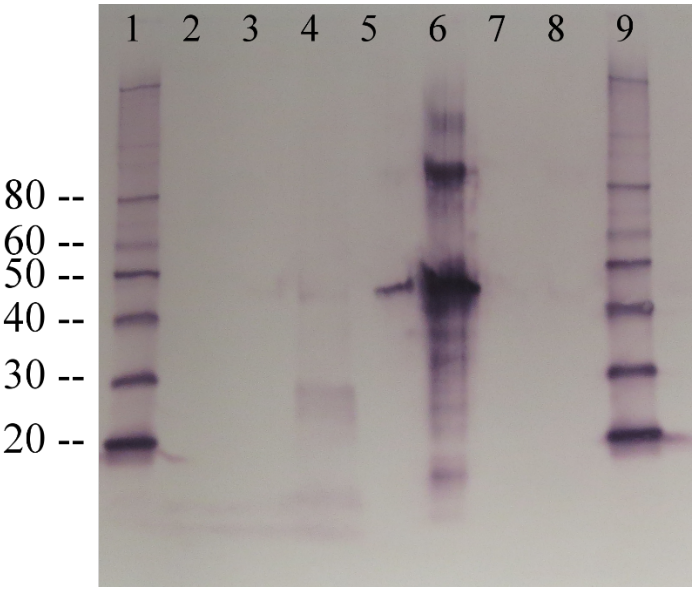

Figure 7. Western blot of purified sunflower fibrils (lane 4) and purified recombinant protein (lane 6) labeled with rabbit anti-sunflower kunitz soybean trypsin inhibitor antibodies. Lane 1 and 9 are MagicMark XP standard ladders.

Previous experiments had shown that the filamentous protein structures were not virus-like. Computational experiments were completed to determine if the major protein coding sequence had any aggregation prone regions indicating it would share similarity with prion-like structures. The portions of a protein sequence that are likely to associate into aggregates through beta strand mediated interactions are limited to short segments which are defined as aggregation-prone regions (APRs) (Betti et al 2016). When analyzed with PLAAC, a prion domain identification algorithm, the SF KTI coding region did not contain Q or N rich regions which many human and fungal prion proteins contain (Figure 8). When analyzed with PrionW no prion-like domains were identified. Tango is a program designed to predict cross-beta sheet aggregation in polypeptide chains (Fernandez-Escamilla et al 2004). It did not predict the presence of beta sheets, beta turns, or beta aggregation in the sunflower KTI polypeptide.

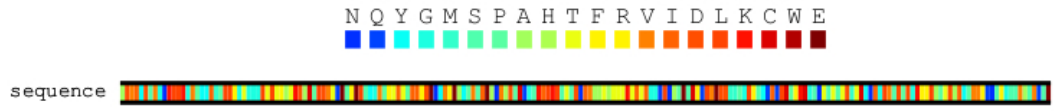

Figure 8. PLAAC (Lancaster et al 2014) results from coding region of sunflower kunitz soybean trypsin inhibitor sequence. Colors represent the amino acids contained in the sequence.

Discussion

Abundant filamentous structures are associated with symptoms of leaf and flower deformation in various plants in the family *Asteraceae*. The filaments are 7-10 nm in diameter and can exceed 3000 nm in length. No encapsidated nucleic acid was detected in the filamentous protein structures as would be expected from a virus-like organism.

However, it is possible the protein may not protect encapsidated nucleic acid (ie: a viral genome). The *potyvirus* group, which contains the thinnest particles among plant viruses, have filaments 12-13 nm in diameter which is much larger than the 7-10 nm diameter of the *Asteraceae* filaments (Kendall et al 2008). Due to their composition of subunit proteins, virus particles also have a distinct helical pitch, which can be observed by TEM (Kendall et al 2008), that is not observed with these filamentous structures. Hereafter these filamentous structures will be referred to as fibrils.

Fibrils purified from sunflower, chrysanthemum, zinnia, and gerbera all have a major protein that migrates with a molecular mass of ~28 kDa during SDS-PAGE. Proteins with other molecular masses are variably associated with the purified fibrils.

N-terminal protein sequencing by Edman degradation was performed on the proteins of fibrils purified from chrysanthemum, gerbera, and zinnia. The N-terminal peptide sequences from the varied sized proteins were nearly-identical. A BLAST search of the EST sequences revealed that the N-terminal sequences had perfect, or almost perfect, identity with predicted mature kunitz-type protease inhibitors (KTI) from chrysanthemum. The mature KTI protein contains a signal sequence that is removed as it is co-translationally inserted into the endoplasmic reticulum lumen. The N-terminal sequences from purified filaments correspond to a region of the mature KTI. This indicates the fibrils are composed of one major protein corresponding to a mature KTI that is present in each of the bands.

To provide further confirmation that the 28 kDa fibril protein is a KTI, the complete coding region of the sunflower KTI with highest identity to the N-terminal

sequences was cloned and sequenced. Then, the proteins of sunflower fibrils were resolved by SDS-PAGE and the four proteins were cut out of the gel, digested with trypsin and sequences of the resulting peptides were obtained by collision-induced dissociation tandem mass spectrometry (CID MS/MS) analysis. The sequence of four of the trypsin fragments had 100% identity with predicted fragments from the cloned sunflower KTI and covered 25% of the sequence. The same three or four trypsin fragments were obtained from each of the differently sized proteins observed by SDS-PAGE. The different size of the protein bands observed by SDS-PAGE could be due to dimerization or degradation of the predicted KTI protein. This is supported by obtaining the same or nearly identical N-terminal and CID MS/MS peptide sequences for different sized proteins composing the filaments.

Antibodies prepared against the cloned sunflower KTI coding region effectively labeled the four protein bands observed from purified sunflower fibrils and the recombinantly expressed protein. Silver staining of SDS-PAGE gels of purified fibril proteins (data not shown) did not identify any other proteins than the major bands observed using Coomassie. It is possible that other minor proteins in very small quantities are associated with the filaments. The repeated isolation of only a single protein with identity to a kunitz soybean trypsin inhibitor protein from fibrils strongly suggests that it is the only major protein comprising the fibrils observed in the *Asteraceae* family.

These data show that the fibrils associated with disease-like symptoms in various members of the family *Asteraceae* are composed of a protein identified as a kunitz soybean trypsin inhibitor. Kunitz soybean trypsin inhibitors (KTIs) are widely distributed

among plants and are often encoded by large gene families ranging in size from two to more than 50 genes (Fischer et al 2015; Islam et al 2015). KTIs are vacuolar-localized and collectively inhibit a wide range of proteases (Fischer et al 2015; Heibges et al 2003; Major & Constabel 2008). In addition, some KTIs have invertase inhibitory activity (Glaczinski et al 2002). Expression of KTIs can be induced by herbivory, wounding, pathogens, abiotic stresses and plant hormones (Kang et al 2002; Kim et al 2003; Li et al 2008). KTIs can be stored proteins and protect plants from herbivory and pathogens (Islam et al 2015; Li et al 2008). At least some KTIs have a role in plant development, since reducing their expression affects leaf shape, shoot growth and root growth (Islam et al 2015; Li et al 2008).

Fibril abundance is highly variable suggesting that it is affected by environmental growth factors that affect KTI expression. Experiments were conducted to determine if treatments known to induce KTI expression (Kang et al 2002; Kim et al 2003; Li et al 2008) to induce high levels of fibrils in sunflowers, however no conclusive conditions were observed. Future experiments challenging the plants with various pests or pathogens may help elucidate the pathways required for the induction of high levels of fibrils. Mechanical inoculation of purified fibrils did not result in an increased level of fibrils in the inoculated plant. There was indication in some species, such as gerbera and coneflower, that the concentration of fibrils was associated with their genotype, some cultivars always had higher levels of fibrils than other cultivars. Fibril levels could range from nearly undetectable to highly abundant as observed by transmission electron microscopy. Only sunflowers with highly abundant fibrils exhibited disease-like

symptoms. As sunflowers aged fibril levels would increase and could be found in both flower petals and leaves. Roots were not tested for the presence of fibrils.

Fibrils composed of host produced protein in animals and fungi can often be composed of amyloid fibrils. Amyloid fibrils are insoluble aggregates of alternately folded cellular proteins that can promote incorporation of the soluble form of the protein into beta amyloid fibrils (Cascarina & Ross 2014; Fowler et al 2007; Newby & Lindquist 2013). Formation of amyloid fibrils causes cell death and is associated with diseases such as Alzheimer's, Huntington's, Parkinson's, and prion diseases (Knowles et al 2014; Ow & Dunstan 2014). In addition to having a negative impact on cellular physiology, amyloid fibrils can also play a beneficial role (Fowler et al 2007; Newby & Lindquist 2013). Amyloid fibrils have been observed and characterized in bacteria, fungi, and animals. Congo red is used as a stain observed by fluorescence microscopy to detect amyloid structures in thin sections of mammal tissue (Puchtler et al 1962). Future experiments could develop a congo red staining protocol suitable for use with purified fibrils to determine if they contain amyloid folds. Thin section experiments (data not shown) did not detect large groups of protein as are detected in mammals with amyloid aggregates (plaques) so it would be necessary to purify the fibrils into a larger concentration for use in congo red experiments.

Aggregation prone regions (APRs) are short segments, 5-15 amino acids in length, of a protein sequence that are susceptible to associating into aggregates of beta-strand-mediated interactions (Rousseau et al 2006). APRs are found in most prions and lead to aggregated beta-sheets (Rousseau et al 2006). Recently, an *Arabidopsis* protein

was identified and shown to have prion-like behavior *in vitro* in a heterologous yeast system (Chakrabortee et al 2016). The coding region of the sunflower KTI was analyzed for amyloid-like aggregation prone regions using three prion prediction algorithms. The algorithms are based on previously described yeast and mammal prion sequences. Neither algorithm identified prion-like domains in the sunflower KTI. Prion-like beta amyloid domains are rich in Q and N and also contain oligopeptide repeats (Chernoff 2004), which are both missing from the sunflower KTI. Tango is a program designed to predict cross-beta sheet aggregation in polypeptide chains (Fernandez-Escamilla et al 2004). It did not predict the presence of beta sheets, beta turns, or beta aggregation in the sunflower KTI polypeptide.

In addition to prions with amyloid folds there are also two fungal prions that do not have amyloid folds. These proteins are classified as prions because they are infectious and self-propagating. *S. cerevisiae* contains the [β] prion which is the self-activating vacuolar protease B (Roberts and Wickner 2003). *P. anserina* contains a non-chromosomal gene called [C] which encodes for protein that is a self-activating mitogen-activated protein (MAP) kinase (Kicka et al. 2006). It is possible that the fibrils composed of plant protein in the *Asteraceae* family are prion-like but do not contain amyloid folds. Protein structure resistance to SDS is another defining feature of prion structures and the *Asteraceae* fibrils could be tested to determine if they are resistant to dissociation by SDS.

Conformational diseases are another diverse group of disorders arising from the conformational structural change of a soluble protein that allows the protein to aggregate

into insoluble aggregates (Carrell & Lomas 1997). Conformational diseases include fibrils and aggregates like haemoglobins sickle cell anemia, prion proteins like Kuru or Creutzfeld-Jakob, serpin family protease inhibitors like antithrombin deficiency thromboembolic disease, and glutamine-repeats like Huntington's as well as amyloidosis (Carrell & Lomas 1997). A feature of conformational diseases is that some level of protein must be correctly folded and released, which then undergoes a conformational change into an alternate form allowing the protein to aggregate into filaments. Conformational diseases do not include genetic diseases that result in the failure to produce a protein (Carrell & Lomas 1997). Further work would be needed to determine the function and native structure of the sunflower KTI to evaluate if it is behaving in a manner similar to these other protein structure aggregation caused disorders.

In addition to the pathological host protein fibrils, it is possible that the KTI protein comprising the *Asteraceae* fibrils has no other native form. The other protein disorders described previously involve the native form of the protein being converted into an alternately folded insoluble form that assembles into fibrils. It is possible that the *Asteraceae* KTI composed fibrils represent a new class of filamentous protein structures that lack similarity to currently described structures. The differences observed in the *Asteraceae* fibrils when compared with known filamentous protein structures indicate further research is required to classify these structures.

It is not known if fibrils have any role in causing the leaf and flower distortion pathologies associated with their presence in high levels. This could be addressed through the creation of sunflower lines with increased KTI expression due to the presence of a

35S:KTI transgene (Sujatha et al 2012). Crisper/Cas9 technology or MicroRNA Induced Gene Silencing (MIGS) could be used to create sunflower mutants that do not express KTI (de Felippes 2013). These two experiments would determine if inhibiting fibril accumulation prevents leaf and flower distortion and if increasing fibril production increases the rate and severity of the leaf and flower distortion.

The results of this project are quite interesting and provide one of the first *in planta* observations of proteinaceous filamentous structures associated with disease-like symptoms. The data indicates the filaments are composed of only one major protein-a kunitz soybean trypsin protease inhibitor. These proteins are normally produced as defense mechanisms or developmental control in plants. Further work is needed to determine if these structures are amyloid-like, prion-like, conformational disease-like, or if they are a new protein aggregation structure unique to the plant kingdom.

Bibliography

Afonso, C. L., Amarasinghe, G. K., Bányai, K., Bào, Y., Basler, C. F., Bavari, S., ... & Bukreyev, A. (2016). Taxonomy of the order Mononegavirales: update 2016. *Archives of virology*, 1-10.

Ahlawat, Y. S., Pant, R. P., Lockhart, B. E. L., Srivastava, M., Chakraborty, N. K., & Varma, A. (1996). Association of a badnavirus with citrus mosaic disease in India. *Plant disease*, *80*(5), 590-592.

Alkowni, R., Zhang, Y. P., Rowhani, A., Uyemoto, J. K., & Minafra, A. (2011). Biological, molecular, and serological studies of a novel strain of grapevine leafroll-associated virus 2. *Virus Genes*, *43*(1), 102-110.

Allen, C., Prior, P., & Hayward, A. C. (2005). *Bacterial wilt disease and the Ralstonia solanacearum species complex*. American Phytopathological Society (APS Press).

Andreas Untergasser, Harm Nijveen, Xiangyu Rao, Ton Bisseling, René Geurts, and Jack A.M. Leunissen (2007). Primer3Plus, an enhanced web interface to Primer3. Nucleic Acids Research, 35: W71-W74; doi:10.1093/nar/gkm306

Arlat, M., Van Gijsegem, F., Huet, J. C., Pernollet, J. C., & Boucher, C. A. (1994). PopA1, a protein which induces a hypersensitivity-like response on specific Petunia genotypes, is secreted via the Hrp pathway of Pseudomonas solanacearum. *The EMBO journal*, *13*(3), 543.

Ball, E. M., Hampton, R. O., De Boer, S. H., & Schaad, N. W., (1990). Polyclonal antibodies. In R. Hampton, E. Ball, and S. De Boer, (eds.), Serological methods for detection and identification of viral and bacterial plant pathogens: A laboratory manual. APS Press. St. Paul Minnesota, U.S.A., pp. 33-54.

Barbara, D. J., & Clark, M. F. (1982). A simple indirect ELISA using F (ab′) 2 fragments of immunoglobulin. *Journal of General Virology*, *58*(2), 315-322.

Betti, C., Vanhoutte, I., Coutuer, S., De Rycke, R., Mishev, K., Vuylsteke, M., ... & Xu, J. (2016). Sequence-specific protein aggregation generates defined protein knockdowns in plants. *Plant physiology*, *171*(2), 773-787.

Blanchfield, A. L., Mackenzie, A. M., Gibbs, A., Kondo, H., Tamada, T., & Wilson, C. R. (2001). Identification of Orchid fleck virus by Reverse Transcriptase-Polymerase Chain Reaction and Analysis of Isolate Relationships. *Journal of phytopathology*, *149*(11-12), 713-718.

Bhat, A. I., Jain, R. K., Kumar, A., Ramiah, M., & Varma, A. (2002). Serological and coat protein sequence studies suggest that necrosis disease on sunflower in India is caused by a strain of Tobacco streak ilarvirus. *Archives of Virology*, *147*(3), 651-658.

Bjerrum, O. J., Selmer, J. C., & Lihme, A. (1987). Native immunoblotting: Transfer of membrane proteins in the presence of non-ionic detergent. *Electrophoresis*, *8*(9), 388-397.

Bombarely, A., Moser, M., Amrad, A., Bao, M., Bapaume, L., Barry, C. S., ... & Bucher, M. (2016). Insight into the evolution of the Solanaceae from the parental genomes of Petunia hybrida. *Nature plants*, *2*, 16074.

Brandle, J. E., Starratt, A. N., & Gijzen, M. (1998). Stevia rebaudiana: its agricultural, biological, and chemical properties. *Canadian journal of plant science*, *78*(4), 527-536.

Burnette, W. N. (1981). "Western blotting": electrophoretic transfer of proteins from sodium dodecyl sulfate-polyacrylamide gels to unmodified nitrocellulose and radiographic detection with antibody and radioiodinated protein A. *Analytical biochemistry*, *112*(2), 195-203.

Carrell, R. W., & Lomas, D. A. (1997). Conformational disease. *The Lancet*, *350*(9071), 134-138

Cascarina, S.M., and Ross, E.D. (2014). Yeast prions and human prion-like proteins: sequence features and prediction methods. Cellular and Molecular Life Sciences *71*, 2047-2063.

Casida, J. E. (1980). Pyrethrum flowers and pyrethroid insecticides. *Environmental health perspectives*, *34*, 189.

Chakrabortee, S., Kayatekin, C., Newby, G. A., Mendillo, M. L., Lancaster, A., & Lindquist, S. (2016). Luminidependens (LD) is an Arabidopsis protein with prion behavior. *Proceedings of the National Academy of Sciences*, 201604478.

Chernoff, Y. O. (2004). Amyloidogenic domains, prions and structural inheritance: rudiments of early life or recent acquisition?. *Current opinion in chemical biology*, *8*(6), 665-671.

Chomczynski, P., & Sacchi, N. (1987). Single-step method of RNA isolation by acid guanidinium thiocyanate-phenol-chloroform extraction. *Analytical biochemistry*, *162*(1), 156-159.

Clark, M. F., & Adams, A. N. (1977). Characteristics of the microplate method of enzyme-linked immunosorbent assay for the detection of plant viruses. *Journal of general virology*, *34*(3), 475-483.

Currier, S., & Lockhart, B. E. L. (1996). Characterization of a potexvirus infecting Hosta spp. *Plant Disease*, *80*(9), 1040-1043.

Dahlin, J. L., Nissink, J. W. M., Strasser, J. M., Francis, S., Higgins, L., Zhou, H., ... & Walters, M. A. (2015). PAINS in the assay: chemical mechanisms of assay interference and promiscuous enzymatic inhibition observed during a sulfhydryl-scavenging HTS. *Journal of medicinal chemistry*, *58*(5), 2091-2113.

Daughtrey, M. L., & Benson, D. M. (2005). Principles of plant health management for ornamental plants. *Annu. Rev. Phytopathol.*, *43*, 141-169.

de Felippes, F.F. (2013). Downregulation of plant genes with miRNA-induced gene silencing. Methods Mol Biol 942, 379-387.

Deahl, K. L., & Fravel, D. R. (2003). Occurrence of leaf blight on petunia caused by Phytophthora infestans in Maryland. *Plant Disease*, *87*(8), 1004-1004.

Doi, Y., Chang, M. U., & Yora, K. (1977). Orchid fleck virus. *CMI/AAB descriptions of plant viruses*, *183*.

Drbal, K., Angelisová, P., Hilgert, I., Černý, J., Novák, P., & Hořejší, V. (2001). A proteolytically truncated form of free CD18, the common chain of leukocyte integrins, as a novel marker of activated myeloid cells. *Blood*, *98*(5), 1561-1566, with modifications by Petr Novak at the Laboratory of Molecular Structure Characterization, Institute of Microbiology, Prague.

Farr, D. F., Bills, G. F., Chamuris, G. P., & Rossman, A. Y. (1989). *Fungi on plants and plant products in the United States*. APS press.

Fernandez-Escamilla, A. M., Rousseau, F., Schymkowitz, J., & Serrano, L. (2004). Prediction of sequence-dependent and mutational effects on the aggregation of peptides and proteins. *Nature biotechnology*, *22*(10), 1302-1306.

Fischer, M., Kuckenberg, M., Kastilan, R., Muth, J., and Gebhardt, C. (2015). Novel in vitro inhibitory functions of potato tuber proteinaceous inhibitors. Mol Genet Genomics *290*, 387-398.

Glaczinski, H., Heibges, A., Salamini, R., and Gebhardt, C. (2002). Members of the Kunitz-type protease inhibitor gene family of potato inhibit soluble tuber invertase in vitro. Potato Res *45*, 163-176.

Gorbalenya, A. E., Donchenko, A. P., Blinov, V. M., & Koonin, E. V. (1989). Cysteine proteases of positive strand RNA viruses and chymotrypsin-like serine proteases. *FEBS letters*, *243*(2), 103-114.

Gorbalenya, A. E., Koonin, E. V., & Wolf, Y. I. (1990). A new superfamily of putative NTP-binding domains encoded by genomes of small DNA and RNA viruses. *FEBS letters*, *262*(1), 145-148.

Gulya, T. & Masirevic, S. (1993). Diseases of Sunflower (*Helianthus annuus* L.) and Jerusalem Artichoke (*H. tuberosus* L.). American Phytopathological Society Common names of plant diseases.
http://www.apsnet.org/publications/commonnames/Pages/Sunflower.aspx

Heibges, A., Salamini, F., and Gebhardt, C. (2003). Functional comparison of homologous members of three groups of Kunitz-type enzyme inhibitors from potato tubers (Solanum tuberosum L.). Mol Genet Genomics *269*, 535-541.

Hogenhout, S. A., Ammar, E. D., Whitfield, A. E., & Redinbaugh, M. G. (2008). Insect vector interactions with persistently transmitted viruses*. *Annu. Rev. Phytopathol.*, *46*, 327-359.

Hu, J. S., Gonsalves, D., Boscia, D., Maixner, M., & Golino, D. (2015). Comparison of rapid detection assays for grapevine leafroll disease associated closteroviruses. *VITIS-Journal of Grapevine Research*, *30*(2), 87.

Hull, R. (2002). *Matthews' plant virology* (4th ed.). San Diego: Academic.

Kadereit, J. W., & Jeffrey, C. (Eds.). (2007). *Flowering Plants. Eudicots: Asterales* (Vol. 8). Springer Science & Business Media.

King, A. M. (2011). *Virus taxonomy: classification and nomenclature of viruses: Ninth Report of the International Committee on Taxonomy of Viruses* (Vol. 9). Elsevier.

Islam, A., Leung, S., Burgess, E.P., Laing, W.A., Richardson, K.A., Hofmann, R.W., Dijkwel, P.P., and McManus, M.T. (2015). Knock-down of transcript abundance of a family of Kunitz proteinase inhibitor genes in white clover (Trifolium repens) reveals a redundancy and diversity of gene function. New Phytol *208*, 1188-1201.

Jones D. T., Taylor W.R., and Thornton J.M. (1992). The rapid generation of mutation data matrices from protein sequences. Computer Applications in the Biosciences 8: 275-282.

Jones, J. B., Stall, R. E., Minsavage, G. V., Dickstein, E. R., Bouzar, H., Roberts, P. D., ... & Engelhard, A. W. (2003). Characterisation of an Acidovorax sp. associated with geranium and petunia. In *Pseudomonas syringae and related pathogens* (pp. 667-673). Springer Netherlands.

Kang, S.G., Choi, J.H., and Suh, S.G. (2002). A leaf-specific 27 kDa protein of potato Kunitz-type proteinase inhibitor is induced in response to abscisic acid, ethylene, methyl jasmonate, and water deficit. Molecules and Cells *13*, 144-147.

Kendall, A., McDonald, M., Bian, W., Bowles, T., Baumgarten, S. C., Shi, J., ... & Havens, W. M. (2008). Structure of flexible filamentous plant viruses. *Journal of virology*, *82*(19), 9546-9554.

Kim, J.S., Kim, Y.O., Ryu, H.J., Kwak, Y.S., Lee, J.Y., and Kang, H. (2003). Isolation of stress-related genes of rubber particles and latex in fig tree (Ficus carica) and their expressions by abiotic stress or plant hormone treatments. Plant Cell Physiol *44*, 412-414.

Kitajima, E. W., Kondo, H., Mackenzie, A., Rezende, J. A. M., Gioria, R., Gibbs, A., & Tamada, T. (2001). Comparative cytopathology and immunocytochemistry of Japanese, Australian and Brazilian isolates of Orchid fleck virus. *Journal of General Plant Pathology*, *67*(3), 231-237.

Ko, N. J., Zettler, F. W., Edwardson, J. R., & Christie, R. G. (1984, June). Light microscopic techniques for detecting orchid viruses. In *VI International Symposium on Virus Diseases of Ornamental Plants 164* (pp. 241-254).

Koenig, R. (1981). Indirect ELISA methods for the broad specificity detection of plant viruses. *Journal of General Virology*, *55*(1), 53-62.

Kondo, H., Maeda, T., & Tamada, T. (2003). Orchid fleck virus: Brevipalpus californicus mite transmission, biological properties and genome structure. *Experimental & applied acarology*, *30*(1-3), 215-223.

Kondo, H., Maeda, T., & Tamada, T. (2009). Identification and characterization of structural proteins of orchid fleck virus. *Archives of virology*, *154*(1), 37-45.

Koonin, E. V., Dolja, V. V., & Morris, T. J. (1993). Evolution and taxonomy of positive-strand RNA viruses: implications of comparative analysis of amino acid sequences. *Critical reviews in biochemistry and molecular biology*, *28*(5), 375-430.

Koonin, E. V., Mushegian, A. R., Ryabov, E. V., & Dolja, V. V. (1991). Diverse groups of plant RNA and DNA viruses share related movement proteins that may possess chaperone-like activity. *Journal of General Virology*, *72*(12), 2895-2903.

Kumar, S., Stecher, G., & Tamura, K. (2016). MEGA7: Molecular Evolutionary Genetics Analysis version 7.0 for bigger datasets. *Molecular biology and evolution*, msw054.

Kumari, A., Kumar, S., & Raj, S. K. (2014). First report of Canna yellow mottle virus on Canna from India. *New Disease Reports*, *29*.

Lancaster, A. K., Nutter-Upham, A., Lindquist, S., & King, O. D. (2014). PLAAC: a web and command-line application to identify proteins with prion-like amino acid composition. *Bioinformatics*, btu310.

Larkin, M. A., Blackshields, G., Brown, N. P., Chenna, R., McGettigan, P. A., McWilliam, H., ... & Thompson, J. D. (2007). Clustal W and Clustal X version 2.0. *bioinformatics*, *23*(21), 2947-2948.

Le Gall, O., Christian, P., Fauquet, C. M., King, A. M., Knowles, N. J., Nakashima, N., ... & Gorbalenya, A. E. (2008). Picornavirales, a proposed order of positive-sense single-stranded RNA viruses with a pseudo-T= 3 virion architecture. *Archives of virology*, *153*(4), 715-727.

Lesemann, D. E. (1996, March). Viruses recently detected in vegetatively propagated Petunia. In *IX International Symposium on Virus Diseases of Ornamental Plants 432* (pp. 88-95).

Li, J., Brader, G., and Palva, E.T. (2008). Kunitz trypsin inhibitor: an antagonist of cell death triggered by phytopathogens and fumonisin b1 in Arabidopsis. Mol Plant *1*, 482-495.

Lin-Moshier, Y., Sebastian, P. J., Higgins, L., Sampson, N. D., Hewitt, J. E., & Marchant, J. S. (2013). Re-evaluation of the role of calcium homeostasis endoplasmic reticulum protein (CHERP) in cellular calcium signaling. *Journal of Biological Chemistry*, *288*(1), 355-367.

Lockhart, B. E., & Mason, S. L. (2011). The Potato Corky Ringspot Pathogen, Tobacco rattle virus, Occurs in Native Habitats in Minnesota. *Plant Health Progress doi*, *10*.

Lockhart, B. E., & Mason, S. L. (2010). First Report of Tobacco rattle virus in Sedum in Minnesota. *Plant Disease*, *94*(3), 374-374.

Lockhart, B. E. L. (2000). Dicentra, Epimedium, and Heuchera: new perennial ornamental hosts of tobacco rattle virus in the United States. *Plant Disease*, *84*(12), 1344-1344.

Lockhart, B. E. L. (1990). Evidence for a double-stranded circular DNA genome in a second group of plant viruses. *Phytopathology*, *80*(2), 127-131.

Ma, B., Zhang, K., Hendrie, C., Liang, C., Li, M., Doherty-Kirby, A., & Lajoie, G. (2003). PEAKS: powerful software for peptide de novo sequencing by tandem mass spectrometry. *Rapid communications in mass spectrometry*, *17*(20), 2337-2342.

Maeda, T., Kondo, H., Mitsuhata, K., & Tamada, T. (1998). Evidence that orchid fleck virus is efficiently transmitted in a persistent manner by the mite *Brevipalpus alifornicus*. 1.13.18. In Abstr., 7th Int. Cong. Plant Pathol. Vol 3., Edinburgh, Scotland.

Major, I.T., and Constabel, C.P. (2008). Functional analysis of the Kunitz trypsin inhibitor family in poplar reveals biochemical diversity and multiplicity in defense against herbivores. Plant Physiol *146*, 888-903.

Mandel, B. (1971). Methods for the study of virus-antibody complexes. *Methods of Virology*, ed. K. Maramorosch, H. Koprowski, pp.375-97.

Margis, R., & Pinck, L. (1992). Effects of site-directed mutagenesis on the presumed catalytic triad and substrate-binding pocket of grapevine fanleaf nepovirus 24-kDa proteinase. *Virology*, *190*(2), 884-888.

Marino, M. T., Ragozzino, E., Lockhart, B. E. L., Miglino, R., & Alioto, D. (2008). First report of Canna yellow mottle virus (CaYMV) in Italy and in the Netherlands. *Plant Pathology*, *57*(2), 394-394.

Mayoa, M. A., & Fritsch, C. (1994). A possible consensus sequence for VPg of viruses in the family Comoviridae. *FEBS letters*, *354*(2), 129-130.

Mei, Y., Bejerman, N., Crew, K. S., McCaffrey, N., & Dietzgen, R. G. (2016). First Report of Orchid fleck virus in Lilyturf (Liriope spicata) in Australia. *Plant Disease*.

Momol, M. T., Lockhart, B. E., Dankers, H., & Adkins, S. (2004). Canna yellow mottle virus detected in Canna in Florida. *Online Plant Health Progress*.

Pataky, N. (1988). Fusarium wilt diseases of herbaceous ornamentals. University of Illinois Extension. RPD No 650, 1-9.

Pearson, W. R., Wood, T., Zhang, Z., & Miller, W. (1997). Comparison of DNA sequences with protein sequences. *Genomics*, *46*(1), 24-36.

Puchtler, H., Sweat, F., & Levine, M. (1962). On the binding of Congo red by amyloid. *Journal of Histochemistry & Cytochemistry*, *10*(3), 355-364.

Ramos-González, P. L., Sarubbi-Orue, H., Gonzales-Segnana, L., Chabi-Jesus, C., Freitas-Astúa, J., & Kitajima, E. W. (2015). Orchid Fleck Virus Infecting Orchids in

Paraguay: First Report and Use of Degenerate Primers for its Detection. *Journal of Phytopathology*.

Redinbaugh, M. G., & Hogenhout, S. A. (2005). Plant rhabdoviruses. In *The World of Rhabdoviruses* (pp. 143-163). Springer Berlin Heidelberg.

Rappsilber, J., Ishihama, Y., & Mann, M. (2003). Stop and go extraction tips for matrix-assisted laser desorption/ionization, nanoelectrospray, and LC/MS sample pretreatment in proteomics. *Analytical chemistry*, *75*(3), 663-670.

Robinson, D. J. (1992). Detection of tobacco rattle virus by reverse transcription and polymerase chain reaction. *Journal of virological methods*, *40*(1), 57-66.

Rose JK, Whitt MA (2001) *Rhabdoviridae*: the viruses and their replication. In: Knipe DM, Howley PM, Griffin DE, Lamb RA, Martin MA, Roizman B, Straus SE (eds) Fields Virology, 4th edn. Lippincott Williams & Wilkins, Philadelphia, pp 1221–1244

Rousseau, F., Serrano, L., & Schymkowitz, J. W. (2006). How evolutionary pressure against protein aggregation shaped chaperone specificity. *Journal of molecular biology*, *355*(5), 1037-1047.

Saitou, N., & Nei, M. (1987). The neighbor-joining method: a new method for reconstructing phylogenetic trees. *Molecular biology and evolution*, *4*(4), 406-425.

Sanchez-Cuevas, M. C., & Nameth, S. G. P. (2002). Virus-associated diseases of double petunia: Frequency and distribution in Ohio greenhouses. *HortScience*, *37*(3), 543-546.

Sanfaçon, H., Wellink, J., Le Gall, O., Karasev, A., Van der Vlugt, R., & Wetzel, T. (2009). Secoviridae: a proposed family of plant viruses within the order Picornavirales that combines the families Sequiviridae and Comoviridae, the unassigned genera Cheravirus and Sadwavirus, and the proposed genus Torradovirus. *Archives of virology*, *154*(5), 899-907.

Shevchenko, A., Wilm, M., Vorm, O., & Mann, M. (1996). Mass spectrometric sequencing of proteins from silver-stained polyacrylamide gels. *Analytical chemistry*, *68*(5), 850-858.

Spooner, D. M., Stimart, D. P., & Boyle, T. H. (1991). Zinnia marylandica (Asteraceae: Heliantheae), a new disease-resistant ornamental hybrid. *Brittonia*, *43*(1), 7-10.

Sujatha, M., Vijay, S., Vasavi, S., Reddy, P.V., and Rao, S.C. (2012). Agrobacterium-mediated transformation of cotyledons of mature seeds of multiple genotypes of sunflower (Helianthus annuus L.). Plant Cell Tiss Org Cult 110, 275-287.

Tomitaka, Y., Usugi, T., Yasuda, F., Okayama, H., & Tsuda, S. (2011). A novel member of the genus Nepovirus isolated from Cucumis melo in Japan. *Phytopathology*, *101*(3), 316-322.

US Department of Agriculture. (2016). Floriculture crops 2015 summary. National Agricultural Statistics Service. Washington, DC. Online: http://usda.mannlib.cornell.edu/usda/current/FlorCrop/FlorCrop-04-26-2016.pdf. Accessed 9 August 2016.

van der Krol, A. R., & Immink, R. G. (2016). Secrets of the world's most popular bedding plant unlocked. *Nature plants*, *2*, 16082.

Van Regenmortel, M. H. V., & Burckard, J. (1980). Detection of a wide spectrum of tobacco mosaic virus strains by indirect enzyme-linked immunosorbent assays (ELISA). *Virology*, *106*(2), 327-334.

Vuong, T. D., Hoffman, D. D., Diers, B. W., Miller, J. F., Steadman, J. R., & Hartman, G. L. (2004). Evaluation of Soybean, Dry Bean, and Sunflower for Resistance to. *Crop Science*, *44*(3), 777-783.

Wijsman, H. J. W. (1982). On the interrelationships of certain species of petunia. *Acta Botanica Neerlandica*, *31*(5-6), 477-490.

Wong, S. M., Chng, C. G., Lee, Y. H., Tan, K., & Zettler, F. W. (1994). Incidence of cymbidium mosaic and odontoglossum ringspot viruses and their significance in orchid cultivation in Singapore. *Crop Protection*, *13*(3), 235-239.

Zambrano, R., Conchillo-Sole, O., Iglesias, V., Illa, R., Rousseau, F., Schymkowitz, J., ... & Ventura, S. (2015). PrionW: a server to identify proteins containing glutamine/asparagine rich prion-like domains and their amyloid cores. *Nucleic acids research*, *43*(W1), W331-W337.

Zettler, F. W., Wisler, G. C., Elliott, M. S., & Ko, N. J. (1987). Some new, potentially significant viruses of orchids and their probable means of transmission. *American Orchid Society bulletin*.

Zettler, F. W., Ko, N. J., Wisler, G. C., Elliott, M. S., & Wong, S. M. (1990). Viruses of orchids and their control. *Plant Disease*, *74*(9), 621-626.

Zheng, G. H., Zheng, Z. Z., Tong, Q. X., & Ming, Y. L. (2013). Orchid fleck virus: an unclassified bipartite, negative-sense RNA plant virus. *Archives of virology*, *158*(2), 313-323.